

University of Windsor

Scholarship at UWindor

Electronic Theses and Dissertations

Theses, Dissertations, and Major Papers

1990

An examination of the force-interval relationship in rat cardiac muscle: Evidence for length modulation of force recovery.

James. Gamble
University of Windsor

Follow this and additional works at: <https://scholar.uwindsor.ca/etd>

Recommended Citation

Gamble, James., "An examination of the force-interval relationship in rat cardiac muscle: Evidence for length modulation of force recovery." (1990). *Electronic Theses and Dissertations*. 1036.
<https://scholar.uwindsor.ca/etd/1036>

This online database contains the full-text of PhD dissertations and Masters' theses of University of Windsor students from 1954 forward. These documents are made available for personal study and research purposes only, in accordance with the Canadian Copyright Act and the Creative Commons license—CC BY-NC-ND (Attribution, Non-Commercial, No Derivative Works). Under this license, works must always be attributed to the copyright holder (original author), cannot be used for any commercial purposes, and may not be altered. Any other use would require the permission of the copyright holder. Students may inquire about withdrawing their dissertation and/or thesis from this database. For additional inquiries, please contact the repository administrator via email (scholarship@uwindsor.ca) or by telephone at 519-253-3000ext. 3208.



National Library
of Canada

Bibliothèque nationale
du Canada

Canadian Theses Service

Service des thèses canadiennes

Ottawa, Canada
K1A 0N4

NOTICE

The quality of this microform is heavily dependent upon the quality of the original thesis submitted for microfilming. Every effort has been made to ensure the highest quality of reproduction possible.

If pages are missing, contact the university which granted the degree.

Some pages may have indistinct print especially if the original pages were typed with a poor typewriter ribbon or if the university sent us an inferior photocopy.

Reproduction in full or in part of this microform is governed by the Canadian Copyright Act, R.S.C. 1970, c. C-30, and subsequent amendments.

AVIS

La qualité de cette microforme dépend grandement de la qualité de la thèse soumise au microfilmage. Nous avons tout fait pour assurer une qualité supérieure de reproduction.

S'il manque des pages, veuillez communiquer avec l'université qui a conféré le grade.

La qualité d'impression de certaines pages peut laisser à désirer, surtout si les pages originales ont été dactylographiées à l'aide d'un ruban usé ou si l'université nous a fait parvenir une photocopie de qualité inférieure.

La reproduction, même partielle, de cette microforme est soumise à la Loi canadienne sur le droit d'auteur, SRC 1970, c. C-30, et ses amendements subséquents.

AN EXAMINATION OF THE FORCE-INTERVAL
RELATIONSHIP IN RAT CARDIAC MUSCLE:
EVIDENCE FOR LENGTH MODULATION
OF FORCE RECOVERY

by

James Gamble

A Thesis

Submitted to the Faculty of Graduate Studies and
Research through the Department of Kinesiology in
Partial Fulfillment of the Requirements for the
Degree of Master of Human Kinetics at the
University of Windsor

Windsor, Ontario, Canada

1990



National Library
of Canada

Bibliothèque nationale
du Canada

Canadian Theses Service Service des thèses canadiennes

Ottawa, Canada
K1A 0N4

The author has granted an irrevocable non-exclusive licence allowing the National Library of Canada to reproduce, loan, distribute or sell copies of his/her thesis by any means and in any form or format, making this thesis available to interested persons.

The author retains ownership of the copyright in his/her thesis. Neither the thesis nor substantial extracts from it may be printed or otherwise reproduced without his/her permission.

L'auteur a accordé une licence irrévocable et non exclusive permettant à la Bibliothèque nationale du Canada de reproduire, prêter, distribuer ou vendre des copies de sa thèse de quelque manière et sous quelque forme que ce soit pour mettre des exemplaires de cette thèse à la disposition des personnes intéressées.

L'auteur conserve la propriété du droit d'auteur qui protège sa thèse. Ni la thèse ni des extraits substantiels de celle-ci ne doivent être imprimés ou autrement reproduits sans son autorisation.

ISBN 0-315-61856-6

Canada

DCP 7287

© James Gamble 1990
All Rights Reserved

AN EXAMINATION OF THE FORCE-INTERVAL RELATIONSHIP
IN RAT CARDIAC MUSCLE: EVIDENCE FOR LENGTH
MODULATION OF FORCE RECOVERY

by

James Gamble

Twitch characteristics were collected at muscle lengths corresponding to 100, 95 and 90% L_{max} . A reduction in muscle length below L_{max} significantly reduced the peak developed force. A progressive reduction in both the positive and negative rates of force development was also found as the muscle was shortened from 100 to 95 and 90% L_{max} .

To determine the influence of muscle length on Ca^{++} handling during interval-dependent force recovery, force-interval data was generated in right ventricular papillary muscles from the rat. This data, coupled with mathematical modelling procedures (Taylor et al., 1989; Schouten et al., 1987), revealed increases of 64% and 99% in the degree of potentiation within the beta process of force recovery as muscle length was reduced to 95% and 90% L_{max} respectively. Similarly, the maximum rate of the beta process was increased by 139% and 197% at 95% and 90% of L_{max} respectively.

Fast-flow buffer exchange experiments were then carried out to determine a mechanism for the length-dependent alteration in the beta process. Subjecting the muscle to a five-fold increase in extracellular Ca^{++} during

121 seconds of rest yielded, at L_{max} , an increase in the degree of potentiation from 3.22 under control conditions to 7.94 following the exchange. At 90% L_{max} , the degree of potentiation increased from 4.61 to 13.54 under control and exchange conditions respectively. A 40% reduction in extracellular Na^+ during rest resulted in increases in the degree of potentiation from 3.21 to 4.02 and from 4.21 to 5.79 at 100% and 90% L_{max} respectively. These disproportionate increases in the exchange experiments between the two muscle lengths suggest that a length-dependent effect on the Na^+/Ca^{++} exchanger exists and may be responsible for the shifts in the beta process of force recovery.

The recirculation fraction of Ca^{++} was determined from the beat to beat decay of potentiation at 100, 95 and 90% L_{max} and yielded values 63, 56 and 55% respectively. This suggests that the recirculation fraction and thus the beat to beat extrusion of Ca^{++} from the cell is also dependent upon the resting muscle length.

DEDICATION

This thesis is dedicated to my dad and mom

ACKNOWLEDGEMENTS

I would like to take this opportunity to extend thanks to those people who assisted me throughout the course of this thesis. In particular I would like to thank Dr. Paul Taylor for his invaluable guidance and his unique motivational techniques that made completion of this thesis a reality. To Dr. Kenji Kenno, my advisor, and Dr. Ray Hermiston each of whose academic input is much appreciated.

I would also like to acknowledge the enormous contributions of Mr. Paul Fazekas which have made completion of this study possible.

Also, to my lab partners Tina McComb and Mark Kontulainen whose help both academically and socially is much appreciated. To my friends back home whose frequent visits and calls made living away from home a little easier.

To my father, for his never-ending support throughout my academic career. Without his direction and contributions the completion of this thesis would never have been possible.

Thank you.

James Gamble

TABLE OF CONTENTS

ABSTRACT	iv
DEDICATION	vi
ACKNOWLEDGMENTS	vii
LIST OF TABLES	ix
LIST OF FIGURES	x
LIST OF APPENDICES	xii
CHAPTER	
I. INTRODUCTION	1
II. METHODOLOGY	
Animal model	12
Muscle preparation	12
Experimental protocol	15
Buffer exchange protocol	21
Data recording	23
Data analysis	23
Statistical analysis	24
III. RESULTS	
Twitch characteristics	25
Force-interval data	31
Potentiation decay	41
Buffer exchange experiments	45
IV. DISCUSSION	
Twitch characteristics	51
Force-interval data	56
Buffer exchange experiments	61
Potentiation decay	68
V. SUMMARY AND CONCLUSION	70
BIBLIOGRAPHY	72
APPENDICES	78
VITA AUCTORIS	104

LIST OF TABLES

1. Twitch characteristic data for right ventricular papillary muscle at 90, 95 and 100% Lmax ...27
2. Twitch characteristic data for right ventricular papillary muscle at 90, 95 and 100% Lmax ...29
3. The influence of resting muscle length on parameters used to characterize the force-interval relationship in right ventricular papillary muscle39

LIST OF FIGURES

1. A) Typical force-interval curve
B) Three-compartment model describing the force-interval relationship of rat ventricular muscle ..7
2. The influence of resting muscle length on the force-interval relationship in rat papillary muscle9
3. Right ventricular papillary muscle mounted between a cradle and force transducer within a muscle bath containing oxygenated KHB buffer ..14
4. Definition of parameters used in the collection of basic twitch characteristics16
5. Protocol used for generation of force-interval data19
6. An overlay of an actual muscle collected from a single muscle at lengths corresponding to 100, 95 and 90% Lmax in 1.0mM Ca++26
7. Raw and fitted force-interval data plotted on a linear x-axis at muscle lengths corresponding to 100, 95 and 90% Lmax32
8. A composite of fitted force-interval data at 100, 95 and 90% Lmax plotted on a logarithmic x-axis ..33
9. Fitted force-interval data at 100% Lmax showing the total curve and also the mathematically isolated alpha and beta processes35
10. Mathematically isolated alpha processes overlayed from each of the three muscle lengths plotted on a logarithmic x-axis36
11. Mathematically isolated beta processes overlayed from each of the three muscle lengths and plotted on a logarithmic x-axis38
12. A) Actual data file showing potentiation decay
B) Linearized potentiation decay plot at 100, 95 and 90% Lmax42
13. The effect of length and Ca++ on rest potentiation in rat papillary muscle45
14. The influence of muscle length and diastolic Ca++ on rest potentiation47

15. The influence of muscle length and diastolic Na ⁺ on rest potentiation	49
--	----

LIST OF APPENDICES

A	- Eyepiece reticle scale used for muscle length measurements	78
B	- Calibration curve for Grass FT03 force transducer	79
C	- Muscle bath developed for buffer exchange experiments	80
D	- Isolated alpha and beta phases - 95% Lmax	81
E	- Isolated alpha and beta phases - 90% Lmax	82
F	- Raw force-interval data - 100% Lmax	83
G	- Raw force-interval data - 95% Lmax	84
H	- Raw force-interval data - 90% Lmax	85
I	- Raw data for twitch characteristics - 100% Lmax ...	86
J	- Raw data for twitch characteristics - 95% Lmax	87
K	- Raw data for twitch characteristics - 90% Lmax	88
L	- Raw data - potentiation decay - 100, 95 and 90% Lmax	89
M	- Eureka fitting procedure values	90
N	- Raw data - buffer exchange experiments - Ca ⁺⁺	91
O	- Raw data - buffer exchange experiments - Low Na ⁺ ..	92
P	- Analysis of variance and Fisher PLSD post hoc analysis	93

INTRODUCTION

The human heart is a muscular pump which serves to deliver blood throughout the cardiovascular system. In order to complete this task, the heart is required, on average, to contract and relax in excess of 100,000 times daily. Each cardiac cycle, consists of muscle shortening and force generation (systole) followed by muscle lengthening and force decay (diastole).

It is only during this diastolic period that blood can enter the ventricles in preparation for delivery during the next contraction phase. The volume of blood filling the ventricles during the diastolic period has a significant influence on the stretch of the myocardium.

Within physiological limits, the stretch on the myocardial wall is dependent upon the degree of ventricular filling during diastole.

Physiologically, the classic studies of Frank and Starling have demonstrated that the greater the degree of diastolic filling (stretch) on the myocardium, the greater the left ventricular output (force production) during systole. This powerful mechanism by which the heart can adjust its force production to alter cardiac output under a variety of acute (ie. exercise, catecholamine release) and chronic conditions (ie. diabetes, hypertrophy, ischemia) is known as the Frank-Starling mechanism or heterometric autoregulation (Lakatta, 1986) and is one of the most

fundamental characteristics of the heart. This ability of the heart to respond to both chronic and acute variations in preload suggests that this phenomenon is an intrinsic property of the myocardium itself (Lakatta, 1977).

Since the early studies of Frank and Starling investigators have attempted to provide a cellular mechanism to describe the effect of myocardial stretch on force development. The observations that a positive relationship exists between intracellular free Ca^{++} and force development (Allen et al., 1974; Wier and Yue, 1986; Reugg, 1986) have focussed attention on two main factors: 1) the effect of muscle stretch on myofilament Ca^{++} sensitivity and; 2) the effect of muscle length on the factors that govern the level of activator Ca^{++} .

It has been well established by a number of physiological studies that the sensitivity of cardiac myofilaments to Ca^{++} increased if the muscle is suddenly lengthened and decreases when the muscle is quickly shortened (Allen and Kurihara, 1982; Hibberd and Jewell, 1982; Kentish et al., 1986; Babu et al., 1988). These data attempt to explain the change in force when the muscle instantly changes its diastolic length. Biochemical studies have determined that at longer versus shorter muscle lengths the affinity of troponin C (a calcium binding protein) is greatly increased which implies that the muscle will ultimately develop greater force. (Hoffman and Fuchs, 1987; 1988).

However, Gordon and Pollack (1980) and Allen et al., (1974) have suggested that the evidence is unclear regarding a length-dependent functioning of the processes that govern the level of activator Ca^{++} . Ridgway and Gordon (1975) have argued that a decrease in Ca^{++} activation at reduced muscle lengths can be attributed to a decrease in the release of Ca^{++} into the myoplasm.

Allen and Kurihara (1982) have analyzed the shape of the calcium transient curve following a sudden reduction in muscle length. They have attributed the decrease in the magnitude and the alteration in the shape of the Ca^{++} transient curve to an decrease in sarcoplasmic reticulum (SR) Ca^{++} release following excitation.

Fabiato et al., (1975), using a skinned ventricular muscle preparation, have shown that the amount of Ca^{++} released from the sarcoplasmic reticulum during calcium-induced calcium release (CICR) varied with the resting muscle length. Their results suggested that more Ca^{++} was released to the myoplasm following excitation at longer lengths than at shorter muscle lengths which may result from a length-dependent change in the effectiveness of Ca^{++} to induce Ca^{++} release from the SR (Fabiato, 1980). However, Jewell (1977) has argued that while muscle length may modulate the function of the SR, it may only play a minor role in the length-dependence of activation.

There are two major concerns however, with the studies attempting to determine the effect of muscle length on the

activation processes. The first, pertains to studies using skinned muscle cells which are considered, by their design, to be non-physiological. While the skinning procedure maintains the integrity of the sarcoplasmic reticulum and myofilaments, it eliminates the contribution of the sarcolemma to the processes of excitation-contraction coupling. This is a particularly important point since Lakatta and Spurgeon (1980) have found evidence that in papillary muscles with intact sarcolemma, the trans-sarcolemmal Ca^{++} influx was length-dependent.

Secondly, it should be pointed out that the majority of studies involving alterations in muscle length have focussed on acute changes that occur immediately following a length change. Little information presently exists on length effects in excitation-contraction coupling under conditions where the muscle is allowed to reach steady-state conditions at each length prior to a given intervention.

Scattered light intensity fluctuations (SLIF), which represent the spontaneous release of Ca^{++} from the SR, also exhibit a steep dependence on muscle length (Lakatta and Lappe, 1981). Given that the frequency of SLIF measurements are known to increase with increased cell Ca^{++} loading (Lakatta, 1986), the above result has been interpreted to indicate that muscle length may influence the degree of cell Ca^{++} loading. However, it should be noted that changes in myofilament Ca^{++} sensitivity now known to occur as a

function of muscle length may also contribute to these results.

In order to gain more information about the influence of muscle length on the integrated contributions of both the sarcolemma and sarcoplasmic reticulum to excitation-contraction coupling, it was necessary to use a more physiological (intact) muscle preparation.

In an attempt to determine whether the processes occurring during excitation-contraction coupling in an intact multicellular preparation were length-dependent, Pogessi et al., (1984) utilized the isolated papillary muscle to examine the phenomenon of post-extrasystolic potentiation at various muscle lengths.

Post-extrasystolic potentiation introduces a premature beat that will result in a stronger subsequent contraction with the degree of potentiation being directly related to the time interval between the premature stimulus and the last steady state event (Pogessi et al., 1984). At shorter muscle lengths the magnitude of the potentiated contraction was further increased (Pogessi et al., 1984) and since muscle length was held constant, suggested that at least one of the steps of excitation-contraction coupling was affected by muscle length. However, they were unable to quantitatively determine which specific event(s) of excitation-contraction coupling was controlled by the muscle length.

A similar method by which the processes of excitation-

contraction coupling can be studied in an intact preparation involves the use of the force-interval relationship. This relationship describes the cellular process whereby force is expressed as a function of the time interval between excitations and has been used to examine intracellular Ca^{++} handling in control (Ragnarsdottir, 1982; Schouten, 1985; Bouchard and Bose, 1989; Johannsson and Asgrimsson, 1988), diabetic (McComb, 1990) hypertrophied (Taylor et al., 1989) and altered thyroid states (Bottinelli et al., 1988) with a wide variety of animal models including guinea pig, ferret, human (Cooper and Fry, 1990; Seed and Walker, 1988; Cooper and Fry, 1988; Arlock et al., 1988), dog (Bouchard and Bose, 1989) and rat (Taylor et al., 1989; McComb, 1990; Gamble, 1990).

If this force-interval response is coupled with a mathematical model of excitation-contraction (E-C) coupling, then quantitative information about the behaviour of cellular calcium can be estimated (Schouten et al., 1987; Taylor et al., 1989).

The most recent model of E-C coupling (Schouten, 1987) was developed to describe the force-interval relationship in rat ventricular muscle (see Figure 1). This model incorporates an uptake and release compartment both presumably located within the sarcoplasmic reticulum and an exchange compartment located at the sarcolemma.

Force generation is therefore thought to involve two

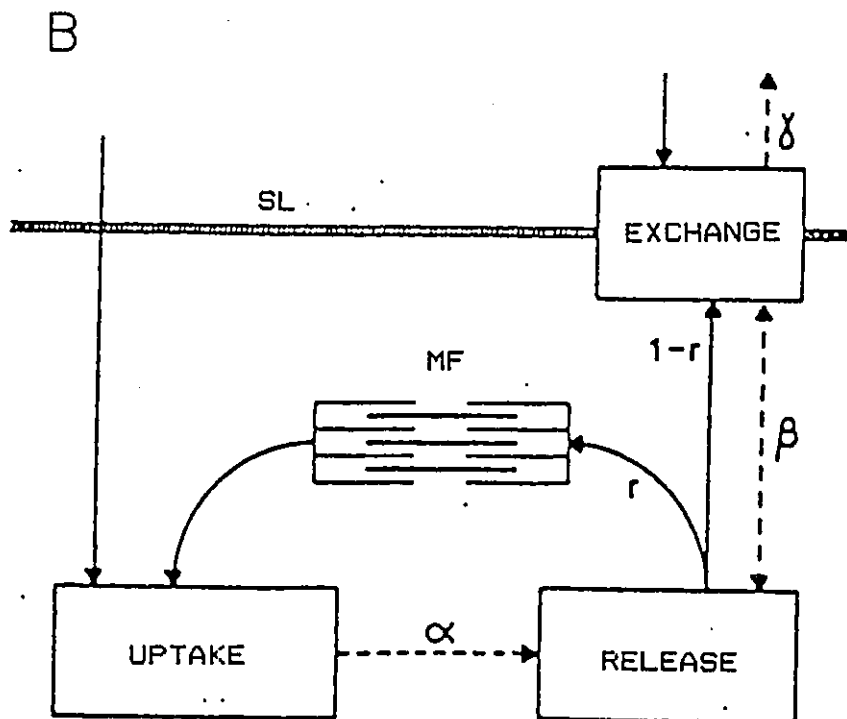
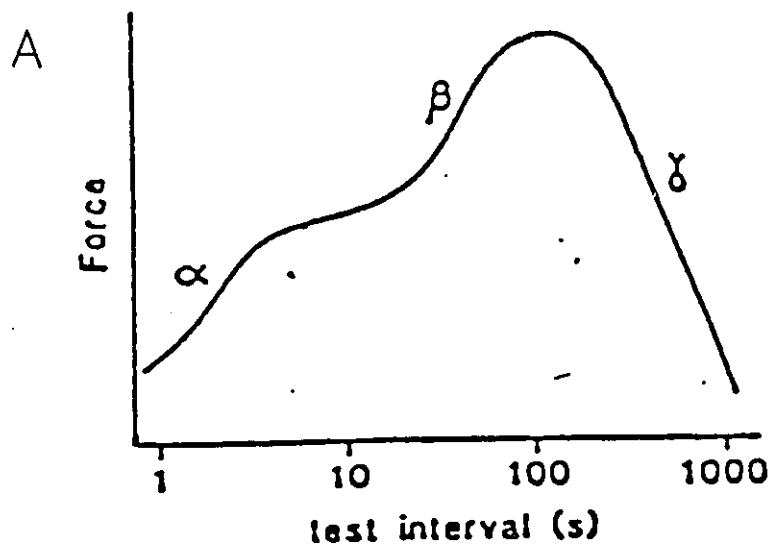


Figure 1. panel A: Typical force-interval curve
 panel B: Three compartment model describing the
 force-interval relationship of rat
 ventricular muscle
 r = recirculation fraction between beats
 $1-r$ = fraction of Ca^{++} extruded with each
 beat
 (Schouten et al., 1987).

simultaneous processes (also termed phases)(Figure 1). The alpha (α) phase represents the time-dependent movement of Ca^{++} between the uptake and release compartments while the beta (β) phase represents the movement of Ca^{++} between the exchange and release compartments.

The third phase, gamma (γ), corresponding to force loss, represents the movement of Ca^{++} from the intracellular space to the extracellular space via the exchange compartment at the sarcolemma.

Thus the experimentally derived force-interval data in conjunction with the mathematical modelling of excitation-contraction coupling gives us insight into the mechanisms by which calcium movements between excitations contribute to the force development on a subsequent beat.

In a pilot study (Gamble, 1990) I have utilized the force-interval data and coupled it with the three compartment model to examine the effect of resting muscle length on intracellular calcium handling. In this study I have extended the initial observations of Pogessi et al., (1984) and demonstrated that muscle length specifically altered the beta phase of the force-interval relationship. More specifically, a progressive increase in force development during the beta phase was found with decreasing muscle length (Figure 2).

In terms of the excitation-contraction coupling model (Schouten et al., 1987), these results indicate that the activity of the beta phase, and therefore the exchange

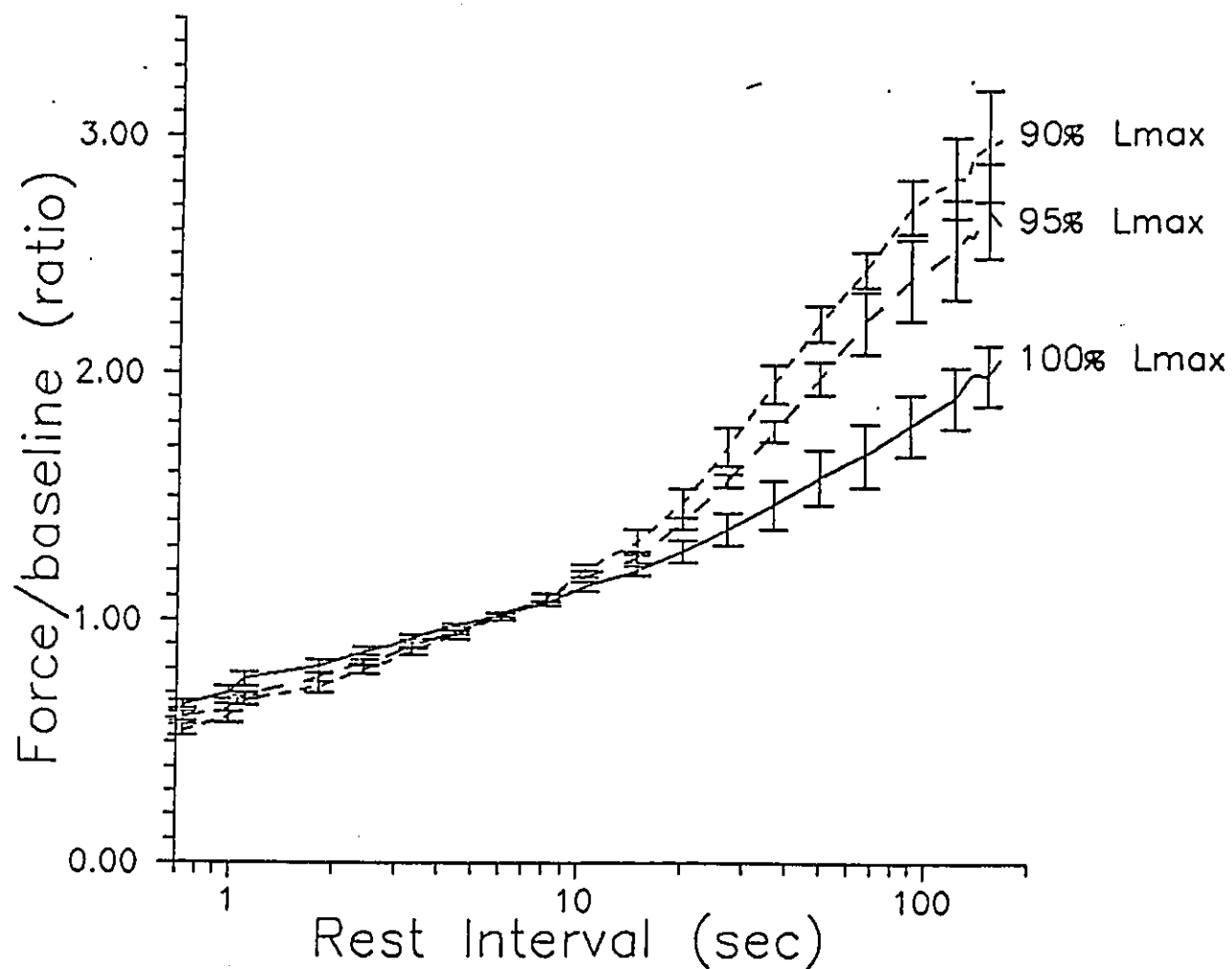


Figure 2. The influence of resting muscle length on the force-interval relationship in rat papillary muscle

compartment, may be length-dependent.

Schouten (1987) has proposed that the beta phase (exchange compartment) may be comprised of the $\text{Na}^+/\text{Ca}^{++}$ exchanger and the Na^+/K^+ ATPase pump. The $\text{Na}^+/\text{Ca}^{++}$ exchanger is a sarcolemmal bound protein which functions electrogenically to primarily extrude calcium ions to the extracellular space in exchange for sodium ions moving into the intracellular space (Reugg, 1986).

However, it is also suggested that the $\text{Na}^+/\text{Ca}^{++}$ exchanger, under certain conditions (ie. long diastolic rest intervals) can reverse its function and promote calcium entry into the cell (Shattock and Bers, 1989). If this is the case, then the muscle should gain more calcium during the long rest interval and the level of expressed force on the next contraction should be increased (Cooper and Fry, 1990; Phillips et al., 1990).

The primary determinants of the function of the exchanger are A): the level of intracellular sodium activity, and B): the concentration of extracellular calcium (Bers, et al., 1988; Bers, 1987; Sonn and Lee, 1988; Sutko et al., 1986). Since it is not possible to directly manipulate the intracellular sodium activity one must therefore manipulate the extracellular sodium and calcium levels in an attempt to alter $\text{Na}^+/\text{Ca}^{++}$ exchange function. Therefore, any net effect on Ca^{++} movements will depend on both the intracellular Na^+ and Ca^{++} activities which exist during the intervention and also the kinetics of the

$\text{Na}^+/\text{Ca}^{++}$ exchange mechanism itself (Sutko et al., 1986).

Therefore based on my pilot study and an extensive review of the current literature, the objectives of this thesis were to:

- A) Determine the effects of muscle length on the basic parameters used to characterize a single twitch in the rat papillary muscle.
- B) To examine the influence of resting muscle length on the intracellular Ca^{++} handling processes associated with excitation-contraction coupling through the use of the force-interval relationship in conjunction with mathematical modelling procedures.
- C) To determine a mechanism to explain the length-dependent changes associated with the force-interval relationship. Specifically, to determine if the $\text{Na}^+/\text{Ca}^{++}$ exchanger is responsible for the length-dependent alterations in the beta phase of the force-interval relationship. This will involve using a fast-flow buffer exchange technique with buffers designed to specifically alter the activity of the exchanger itself.

METHODS

Animal Model

Male Wistar rats (190-220g) (Charles River, Que.) were housed in a temperature (23°C) and light-controlled (12:12 hour light-dark cycle) animal facility at the Faculty of Human Kinetics, University of Windsor, according to the guidelines set forth by the Canadian Council on Animal Care. Water and Purina lab chow were provided for the animals ad libitum.

Muscle Preparation

At the time of sacrifice the animals were ether anaesthetized and injected with 107 units of heparin (Sigma) per kilogram body weight via the inferior vena cava to prevent blood clotting. The hearts were then rapidly excised, placed in ice cold saline and transferred to a dissection chamber. The aorta was cannulated and then perfused at a flow rate of 10 ml/min with a modified Krebs-Henseleit bicarbonate buffer containing the following salts (in mM): NaCl, 117.1; KCl, 5.0; MgCl₂ · 6H₂O, 1.2; Na₂SO₄, 2.4; NaH₂PO₄ · 2H₂O, 2.0; NaHCO₃, 27.0; glucose, 10; CaCl₂, 1.0. This perfusate was oxygenated at room temperature with 95% O₂ : 5% CO₂ to obtain a pH of 7.4.

It has been shown that with a Ca⁺⁺ concentration of 2.5mM, one or more of the calcium dependent force generating mechanisms is saturated and force generation is maximal (ter Keurs et al., 1980; Forester and Mainwood,

1974) All of the force recovery data were therefore collected at 1.0mM Ca^{++} to avoid saturation of the calcium kinetics and to allow both phases of force generation to be examined.

Following a washout period, 10 ml KCl ([final] = 15 mM) was added to the perfusate to arrest beating. Using a dissecting microscope, the right ventricle was opened and the free wall pulled back to expose the papillary muscles according to the method of ter Keurs et al. (1980) for trabeculae. Only long thin papillary muscles with uniform sides and no branches were selected for study. These muscles have a more uniform sarcomere spacing throughout their length and will generate force in direct line with the force transducer. A portion of the tricuspid valve was excised with the papillary muscle and a hole was placed in it for mounting purposes.

The papillary muscle was then transferred to a muscle bath located on the stage of a dissecting microscope and perfused with the modified Krebs-Henseleit buffer ($[\text{Ca}^{++}] = 1.0\text{mM}$) at 26°C . This temperature, although not physiological, allowed the preparation to be more stable over the course of the experiment. (Taylor, 1989 personal communication). The muscle was mounted horizontally with the portion of the ventricular wall surrounding the base of the papillary muscle suspended in a cradle and the tricuspid valve at the opposite end placed over a tungsten wire hook which was attached to the arm of a force

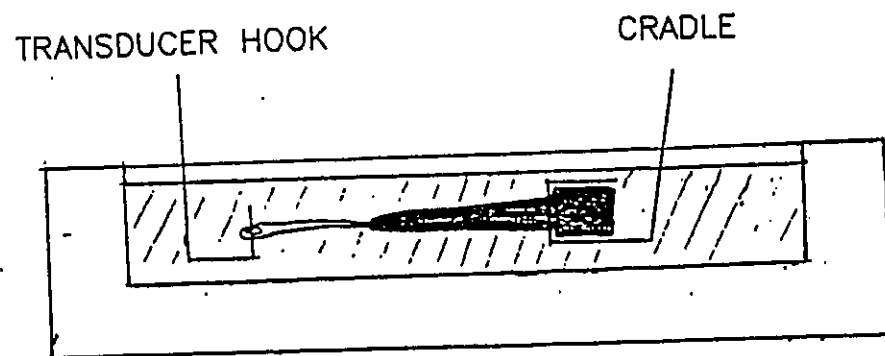


Figure 3. Right ventricular papillary muscle mounted between a cradle and force transducer within a muscle bath containing oxygenated KHB buffer.

transducer (Grass FT03) (see Figure 3).

The muscle was stimulated (Grass S6 C) at 150% threshold via two platinum wire electrodes located perpendicular to the long axis and on either side of the muscle. This stimulation voltage was determined by increasing the voltage until a contraction was seen then increasing that voltage by 50%. Both the pacing frequency and the various rest intervals were under microcomputer control.

A moderate load was established and the muscle was allowed to equilibrate for 60 minutes at a pacing frequency of 1.0 Hz. This stimulation frequency during equilibration was found to increase the stability of the preparation during the course of the experiment. The equilibration period itself is necessary to allow the muscle to recover from the surgery and equilibrate to the Ca^{++} concentration. Following equilibration, the muscle was paced at 0.2Hz (1 beat every 5 seconds) and the muscle length was then increased gradually using a micromanipulator to establish L_{max} (ie. the muscle length that elicits the greatest active force).

Experimental Protocol

Following the establishment of L_{max} , a data file was collected at a Ca^{++} concentration of 1.0 mM and 26 °C to obtain basic twitch characteristics.

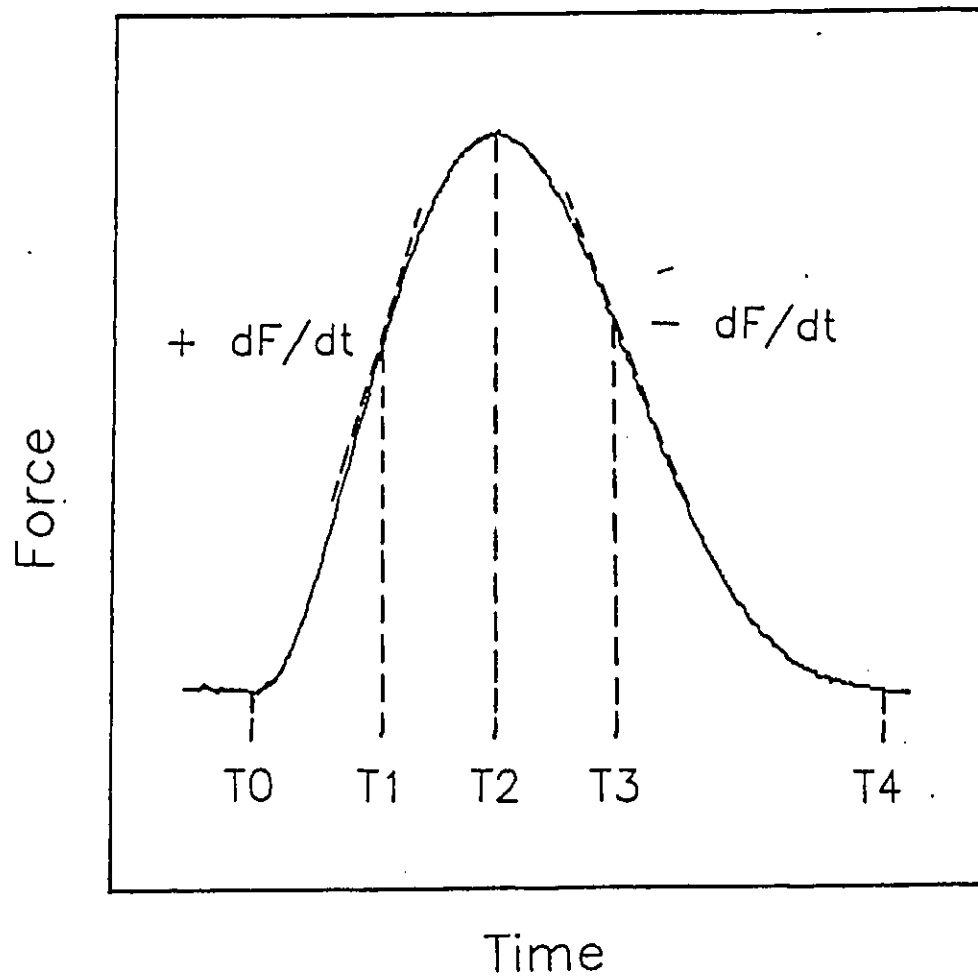


Figure 4. Definition of parameters used in the collection of basic twitch characteristics.

Figure 4 displays a general twitch function curve for the right ventricular papillary muscle and defines the various parameters used to characterize each function. Immediately prior to contraction, the muscle produces a given level of passive tension or baseline force development. At the initiation of contraction, the force rises rapidly and smoothly from the baseline to a level of peak tension development. From this point, the force decreases more slowly until it once again returns to the baseline.

The twitch curve therefore contains two phases. A contractile phase which composes the ascending limb and a relaxation phase consisting of the descending portion of the curve. It is also evident from Figure 4 that the relationship between these two phases is such that the curve is asymmetrical. The contractile response being much faster than that of relaxation which is more prolonged.

From these function curves, one can generate two types of information. First, various measures of force can be derived such as peak force, both the positive and negative maximum rates of force development ($\pm dF/dt$) and the ratio of these two maximum rates ($S+/S-$).

Secondly various timing parameters can be precisely examined within both the contraction and relaxation phases. During the contractile phase, one can measure the time required to reach peak force development (T_0-T_2), the time necessary to achieve the maximal positive rate of force

development (T0-T1) and the time from the maximal positive rate to peak developed force (T1-T2).

In the descending limb of the of the function curve, one can derive the time from peak tension to complete relaxation (T2-T4), time from peak tension to the position of maximal rate of force decay (T2-T3) and finally, the time from the maximal relaxation rate to complete relaxation (T3-T4).

Twenty-four rest intervals were used (0.40, 0.54, 0.73, 0.99, 1.34, 1.81, 2.44, 3.30, 4.46, 6.02, 8.13, 10.47, 14.81, 20.00, 27.00, 36.45, 49.21, 66.44, 89.70, 121.0, 130.00, 135.00, 150.00, and 163.00 secs) in generating the force-interval data. These rest intervals were chosen to allow full examination of both force generating phases of the force-interval relationship.

A viable preparation was characterized by a stable baseline force development, no aftercontractions and no spontaneous contractions. Those muscles exhibiting one or more of these characteristics were discarded. On average, approximately 75% of the excised papillary muscles (not including those hearts with no appropriate muscles) were considered to be stable and viable preparations.

The control pacing frequency of 0.2Hz was used between rest intervals until the steady-state force had stabilized. The beat immediately prior to the rest interval was collected as the control beat with the first beat following the rest interval recorded as the test contraction (Figure

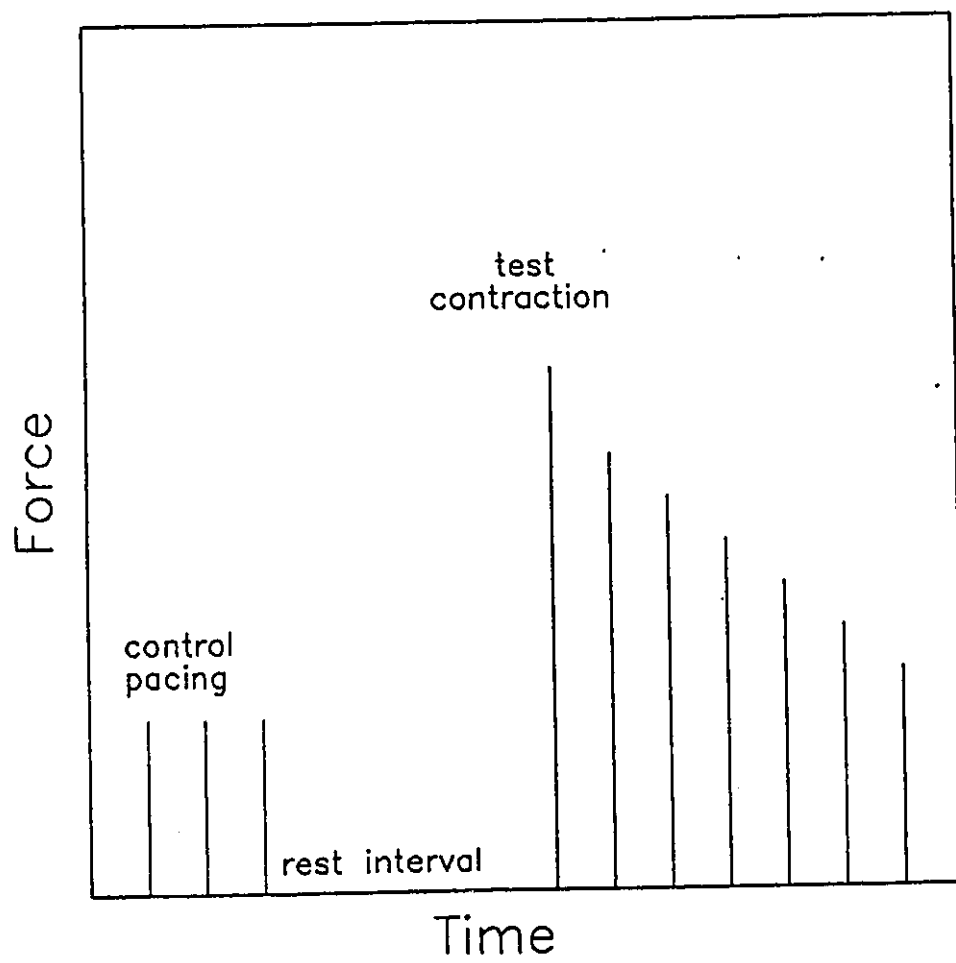


Figure 5. Protocol used in the generation of force-interval data.

5). Force-interval curves were then generated by plotting the developed force of the test beat as a ratio of the force development on the control beat (force/baseline) as a function of the rest interval. During data collection, rest intervals were only imposed when the force development during control pacing had become stable.

Once the force-interval data was collected at L_{max} , the muscle was adjusted to a percentage of L_{max} (0.95, 0.90) through the use of an eyepiece reticle scale (appendix A). These percentages have been shown to represent a range of sarcomere lengths of approximately 2.25 μ m to 2.10 μ m and a developed force range of approximately 100% to 50% respectively in rat papillary muscle (Pollack and Huntsman, 1974).

The distance between the hook and the edge of the cradle, as measured by the eyepiece reticle, at L_{max} was recorded as 100% with the experimental lengths being taken as a fraction of this distance.

Once the new muscle length had been established, the muscle was allowed to equilibrate for a period of twenty minutes. Twitch characteristics were then collected for the new length. The test intervals were once again imposed on the muscle and the data were collected as previously described. As many muscle lengths as possible were imposed on the muscle provided that the preparation remained stable and maintained significant force development. For the data presented in this thesis, each muscle was subjected to all

three of the muscle lengths chosen for investigation. Therefore, each muscle served as its own control.

In order to collect data for the analysis of potentiation decay in 1.0 mM Ca^{++} following the 121.0 second rest interval, it was necessary to increase the total number of data points collected per file to 2000. Therefore by sampling 250 points per curve this allowed a total of eight curves to be used in the decay analysis.

Rapid flow buffer exchange technique

The buffer exchange protocol involved a dissection and stabilization protocol identical to that outlined above. However, it was necessary to design and build, in the laboratory, a muscle bath that would allow for a much faster flow and exchange of buffer over the surface of the muscle. This involved designing a muscle chamber whose total volume was very small and whose dimensions would direct the buffer, at a high flow rate, (20 ml/min) directly over the tissue and reduce the pooling of the residual buffer within the bath (appendix C).

Three special flow tubes, each of which delivered a buffer of different ionic composition, were positioned at one end of the chamber directly in front of the valvular end of the papillary muscle. The base of the chamber was cut at an angle to facilitate buffer flow across the muscle and into a collecting pool located at the opposite end of the chamber. This collecting pool served as a reservoir for

the residual buffer until it was removed via a sipper tube and also eliminated buffer contamination problems by restricting any backflow of buffer into the muscle chamber.

In order to determine whether the activity of the exchange compartment, ie. $\text{Na}^+/\text{Ca}^{++}$ exchanger, was length dependent, the rest interval of 121.0 seconds was chosen because this time was found to produce near maximal potentiation in the pilot study. This protocol involved stabilizing the muscle and determining 100% L_{max} in 1.0mM Ca^{++} followed by a data file at 121.0 seconds to confirm that the muscle was representative of those in the pilot study.

Following this, the Ca^{++} concentration was reduced to 0.5mM (in order to maximize the Ca^{++} gradient during the buffer exchange experiments to follow later) and the muscle was allowed to stabilize. The muscle was then subjected to a 121.0 second rest period and a data file was collected. The next data file that was collected was the buffer exchange file. This involved switching the buffer perfusing the muscle during the 121.0 second rest period to one containing either 2.5mM Ca^{++} or 70.26 mM Na^+ (ie. 40% reduction). In order to maintain the osmotic balance of the cell, an equimolar amount of LiCl (46.84mM) was added to the perfusate during the Na^+ reduction experiments. These values were chosen to maximize any alterations that may have been present.

The muscle length was then reduced to 90% L_{max} using

the eyepiece reticle scale, data files were collected as stated above.

Data Recording

Force signals generated by the transducer were amplified by a Grass preamplifier (model 7P122D) powered by a Grass power supply (RPD 107E). This signal was then converted to digital form using a 12-bit analogue-digital (A-D) converter. Sampling rate was set at 250 microseconds with each twitch curve representing a minimum of 250 data points. This data was then analyzed by a microcomputer program and stored on floppy disk.

Data Analysis

The following timing parameters were used to describe the twitch characteristics performed in 1mM Ca⁺⁺: time to peak tension (T0-T2), time to complete relaxation (T2-T4), time to half maximal force development (T0-T1), time for half maximal to maximal force development (T1-T2), time to half relaxation (T2-T3) and time from half relaxation to complete relaxation (T3-T4).

The force parameters included peak isometric developed tension, positive rate of force development ($+ dT/dt$), maximum rate of relaxation ($- dT/dt$), and the ratio of rates of force generation and relaxation ($S+/S-$).

Force recovery curves were generated by plotting the force development of the test contraction (as a ratio of the baseline force production derived from the control beat immediately prior to the rest interval ie. force/baseline) versus the rest time. This method provided a more stable force value and was less affected by a reduction in force over time since developed force was compared to the force developed on the beat immediately prior to the test interval.

The force-interval data were fitted to a mathematical model that using a nonlinear, recursive, least squares analysis which allowed detailed characterization of the force-interval curves (Taylor et al., 1989).

$$f(t) = F_{\text{end}} * (1 - M * \exp(-at) - (1 - M) * \exp(-bt))$$

In particular, the characterization involved calculation of maximum rates, time constants, and percent contribution of each force generating phase (alpha and beta) of the force-interval relationship.

Statistical analysis

An analysis of variance (ANOVA) with repeated measures was used in conjunction with a Fisher post hoc analysis test to determine whether statistically significant differences were present between levels of the independent variable. The level of significance was set at $p < 0.05$.

Results:

1. Twitch characteristics

In this study twitch characteristics were collected at each of three muscle lengths corresponding to 100, 95 and 90% Lmax. The resting muscle length had a significant influence on a number of the parameters used to characterize the muscle twitch. Visually, Figure 6 illustrates an overlay of twitches taken from a single muscle at 100, 95 and 90% Lmax. Qualitatively, muscle length has a strong influence on the magnitude and shape of the twitch function curve.

Listed in Table 1 are the various quantitative force parameters used to characterize single twitches at 100, 95 and 90% Lmax. The peak developed tension, normalized by muscle cross-sectional area, was significantly reduced at the lower muscle lengths relative to 100% Lmax. Although not statistically different from each other, the peak developed tension at 95 and 90% showed a trend towards being reduced with decreasing muscle length. On the other hand, the maximum rates of force development ($+dF/dT$) and relaxation ($-dF/dT$), were significantly reduced at 95 and 90% of Lmax.

The ratio of the positive to negative maximum rates of force development ($S+/S-$) revealed a progressive reduction with decreasing muscle length. Relative to Lmax, this ratio was reduced by 18% and 29% at 95% and 90% Lmax respectively.

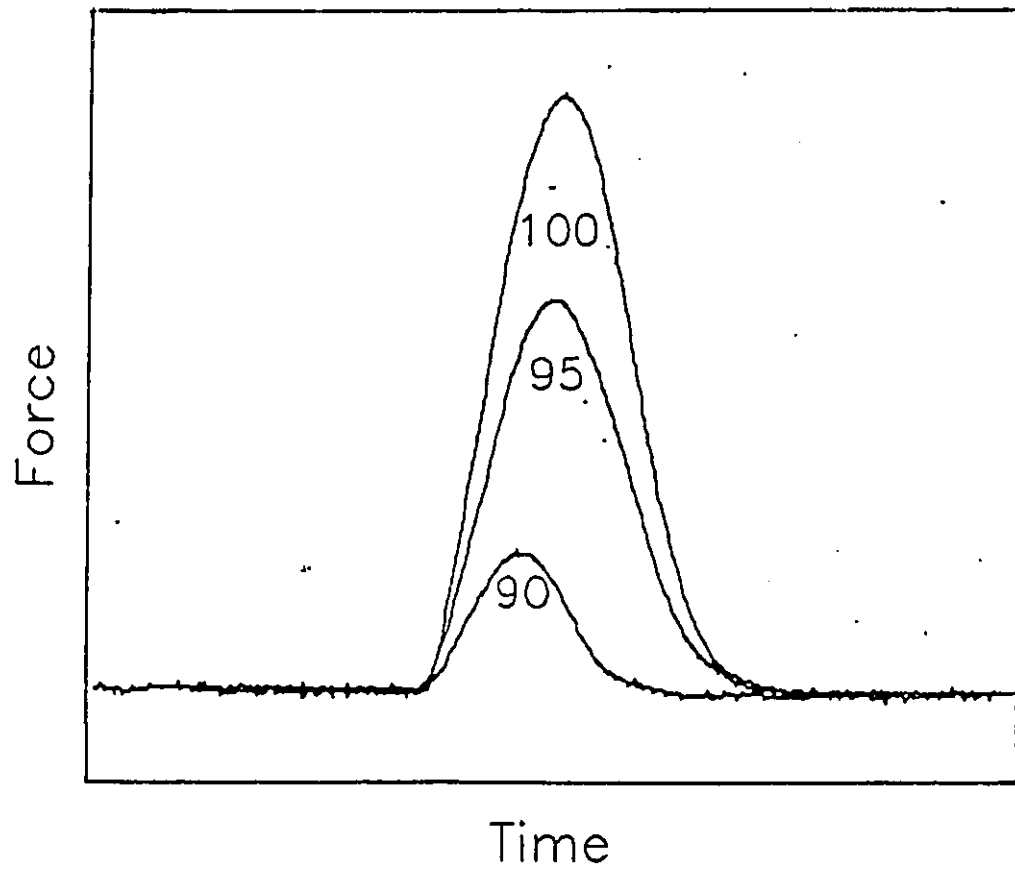


Figure 6. An overlay of an actual muscle twitch collected from a single muscle at lengths corresponding to 100, 95 and 90% L_{max} in 1.0mM Ca^{++} .

Table 1. Twitch characteristic data for right ventricular papillary muscle at 90, 95 and 100% of Lmax.

FORCE PARAMETER	MUSCLE LENGTH (% Lmax)		
	100	95	90
TENSION (mN/mm ²)	41±9	10±3*	4±1*
+ dF/dt (mN/sec/mm ²)	191±22	110±29*	60±15*#
- dF/dt (mN/sec/mm ²)	115±14	79±19*	47±9*#
S+/S-	1.7±.1	1.4±.1*	1.2±.1*#

* sig. from 100% p < .05

sig. from 95% p < .05

S+/S- represents the ratio of the positive and negative rates of force development

Values represent the means ± SE of five animals.
The external calcium concentration was 1.0mM and the muscles were paced at 0.2 Hz.

From these results, one might suggest that the processes associated with activation/contraction and relaxation are not uniformly influenced by the resting muscle length.

As shown quantitatively in Table 2, the resting muscle length had a significant influence on a number of timing parameters. Within the contractile phase, a reduction in muscle length below L_{max} significantly reduced the time required to achieve maximal force development (T_0-T_2). At 95 and 90% L_{max} , respectively, there was a 26% and 33% reduction in the time to peak tension. Resting muscle length was found to have no effect on the early portion of force development (T_0-T_1) but did result in a significant 40-48% reduction in the T_1-T_2 segment as muscle length was reduced to 95 and 90% L_{max} .

Within the relaxation phase, there was a progressive reduction in total relaxation time (T_2-T_4) as muscle length was reduced from L_{max} . Specifically, at 95% L_{max} the total relaxation time decreased by 37% while a reduction by 51% was found as the muscle length was reduced to 90% L_{max} .

The time required for the muscle to relax from peak tension to the maximal relaxation rate was also found to decrease with a reduction in muscle length from L_{max} . While no statistically significant differences were found, the muscles at 95 and 90% L_{max} showed a 35% and 48% reduction respectively, for the T_2-T_3 values as compared to optimal length which may be considered significant decreases from a physiological standpoint. A reduction in the time required

Table 2. Twitch characteristic data for right ventricular papillary muscle at 90, 95 and 100% of Lmax.

TIME PARAMETER SEGMENT	MUSCLE LENGTH (% Lmax)		
	100	95	90
CONTRACTION PHASE:			
T0 - T2 (msec)	187 \pm 6	138 \pm 9*	125 \pm 8*
T0 - T1 (msec)	53 \pm 3	58 \pm 2	62 \pm 4
T1 - T2 (msec)	134 \pm 6	80 \pm 8*	69 \pm 6*
RELAXATION PHASE:			
T2 - T4 (msec)	375 \pm 11	236 \pm 24*	185 \pm 15*#
T2 - T3 (msec)	116 \pm 10	75 \pm 7*	64 \pm 5*
T3 - T4 (msec)	259 \pm 19	141 \pm 29*	125 \pm 11*

* sig. from 100% p < .05

sig. from 95% p < .05

Values represent the means \pm SE of at least five animals. The external calcium concentration was 1.0mM and the muscles were paced at 0.2 Hz.

T0 = baseline

T1 = max. rate of force development

T2 = peak developed force

T3 = max. rate of relaxation

T4 = baseline

to complete the late portion of the relaxation phase, T3-T4, was also evident. A 37% reduction for this segment was found at 95% Lmax as compared to optimal length, with a more pronounced reduction of 51% when the muscle length was set at 90% Lmax.

It is interesting to note that given the very similar percent reductions (~50%) at 90% Lmax versus 100% Lmax for the T1-T2 segment of the contractile phase and all of the segments of the relaxation phase, a similar mechanism or series of processes may be responsible for these alterations whose activity is a function of the resting muscle length.

2. Force-Interval

Force-interval curves were derived by plotting the ratio of the developed force on the test beat and the force of the beat immediately prior to the rest interval as a function of the rest interval itself. In order to insure that the fitted parameters reflected the raw data, Figure 7 compares the force-interval response of the experimentally derived data with the fitted curves at all three muscle lengths. The data clearly show that the parameters selected for the mathematical fit correspond extremely well with the raw data.

The data in Figure 8 are a log transformation of the force-interval data at 90, 95 and 100% L_{max} . These results clearly show that force recovery is a biphasic function which has been identified as alpha and beta respectively (Schouten et al., 1987). In other words, force recovery between beats is not the result of a single process.

From these data, it is evident that the muscle length did result in alterations in both the alpha and beta phases. The alpha phase, occurring at rest intervals up to approximately 10 seconds, is slightly depressed at muscle lengths less than L_{max} . In contrast, the beta phase, occurring at rest intervals up to approximately 160 seconds, became progressively more dominant as muscle length was reduced below L_{max} . Specifically, this resulted in progressive increases in the maximum degree of potentiations (calculated from the peak of the force-

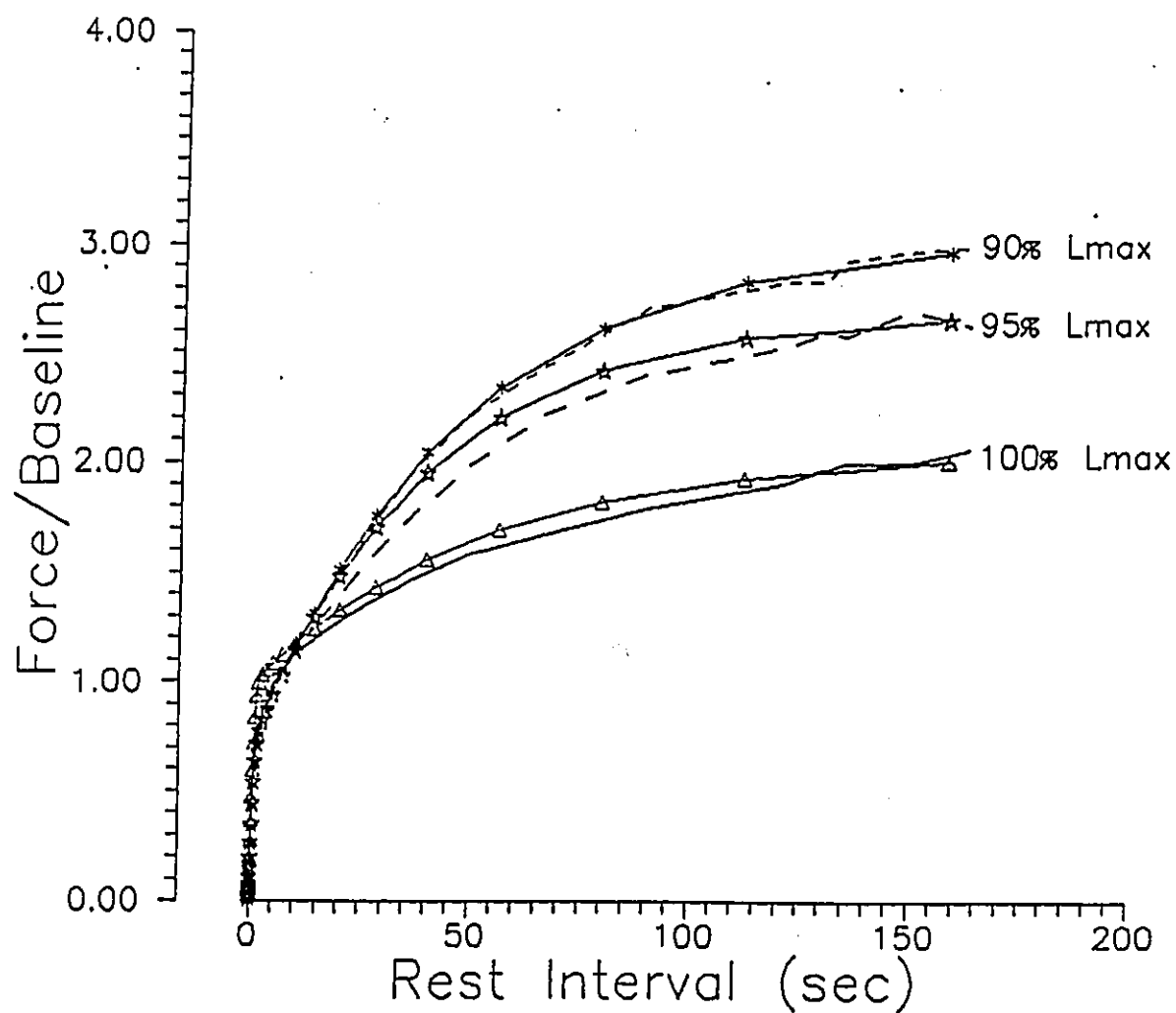


Figure 7. Raw (no symbols) and fitted (centered symbols) force-interval data plotted on a linear x-axis at muscle lengths corresponding to 100, 95 and 90% Lmax.

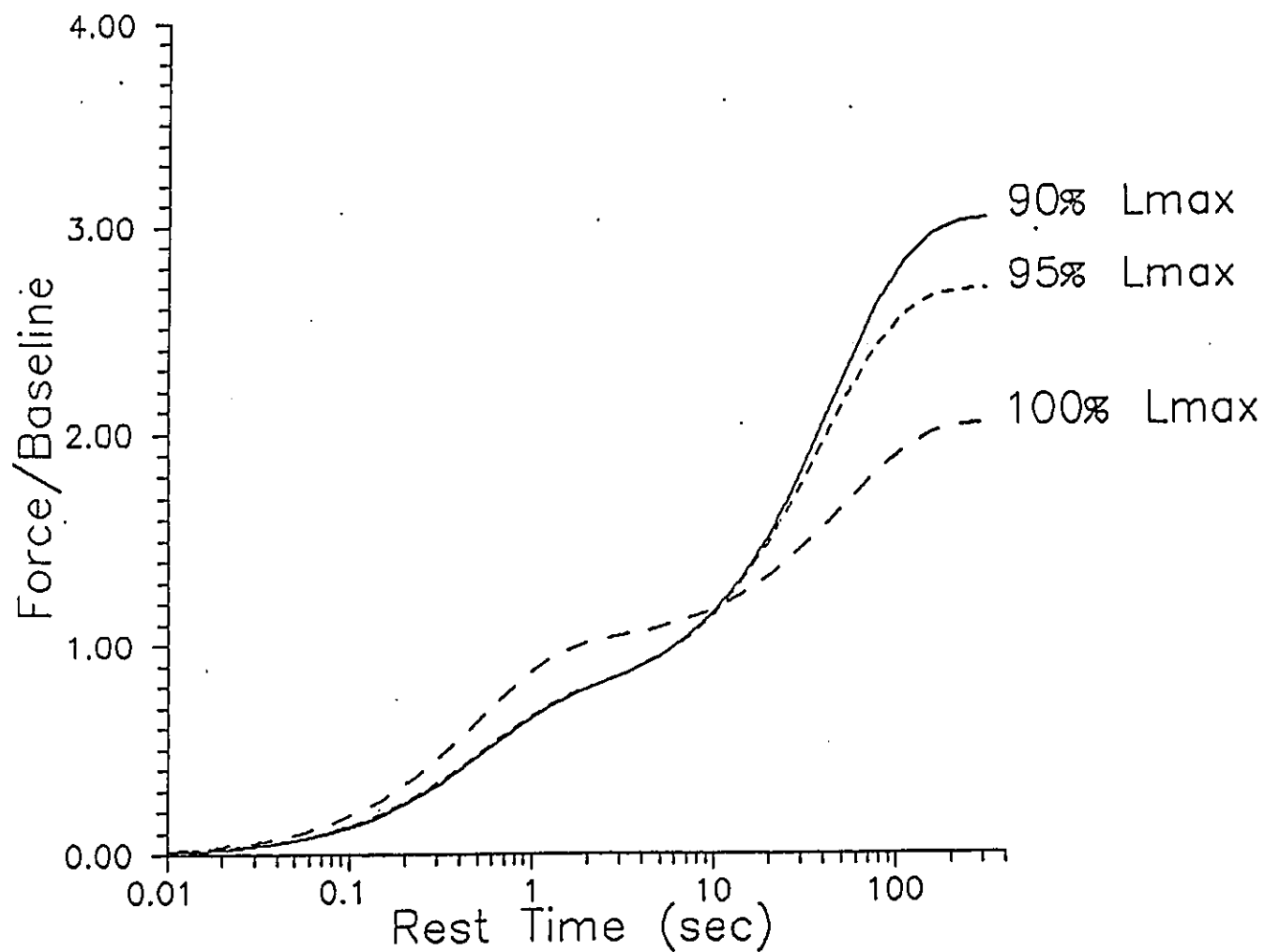


Figure 8. A composite of fitted force-interval data at 100, 95 and 90% Lmax plotted on a logarithmic x-axis.

interval curve) from 2.04 at L_{max} to 2.68 and 3.03 at 95 and 90% respectively (Table 3).

To more fully characterize the effect of muscle length on interval-dependent force recovery it was necessary to isolate each process from the complete curve and then quantitatively analyze each component (alpha and beta).

The fitted data in Figure 9 illustrate the isolation of each process plotted on a logarithmic time axis. According to the model that was used, each process was activated at time zero and then evolved with increasing diastolic rest intervals. How these processes evolve with time is determined by the cellular mechanisms that influence each component. In general it can be observed that the process alpha contributes earlier than the beta component.

In order to more clearly examine the effect of muscle length on the isolated alpha and beta processes, I have plotted each phase at 100, 95 and 90% L_{max} .

Visual inspection of Figure 10 shows that muscle length had a pronounced effect on the alpha process of force recovery. At the shorter muscle lengths, the process is shifted to the right and the plateau (amplitude) appears to be depressed.

To more accurately characterize the influence of muscle length on the alpha process, this component was quantified in terms of its time constant, maximum rate and its percent contribution to the total force recovery. From

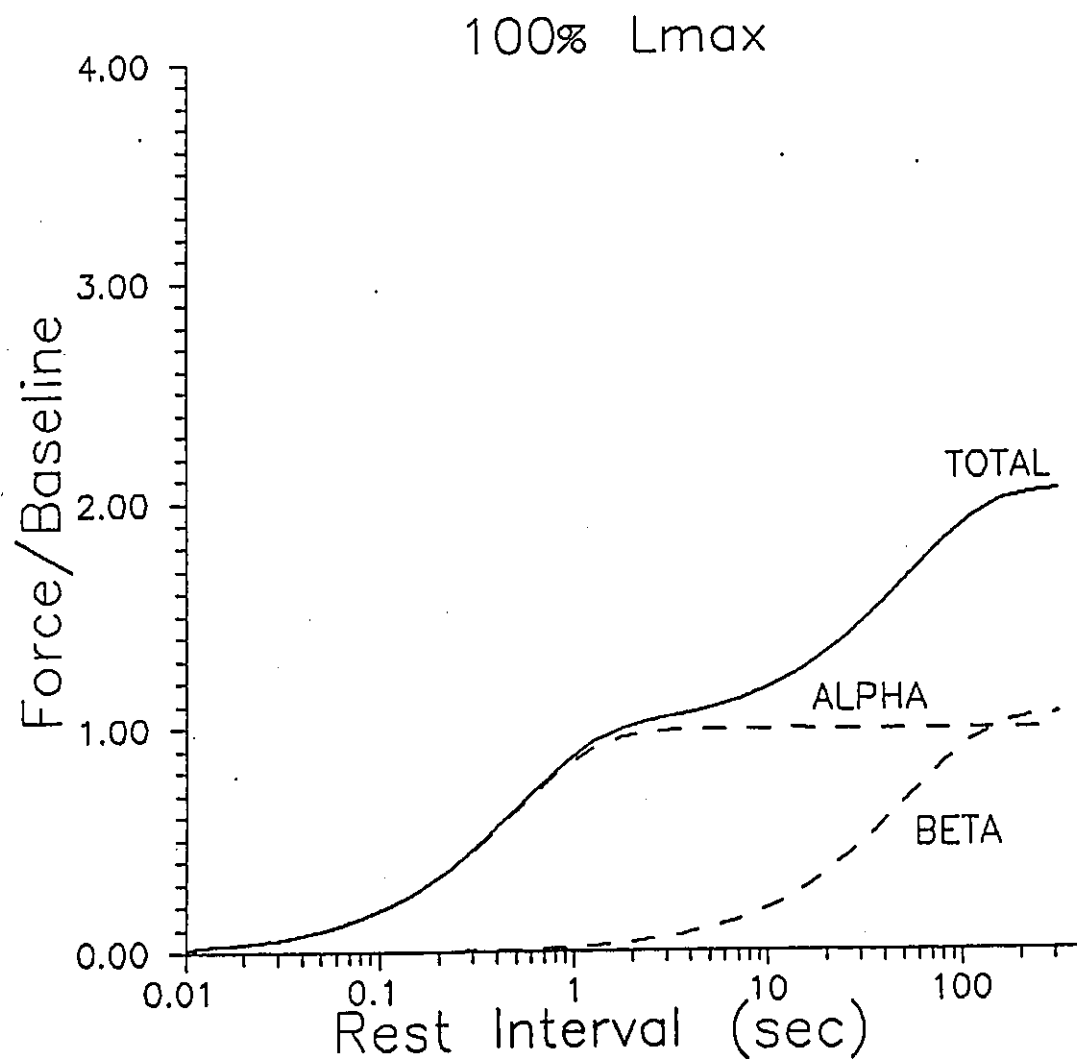


Figure 9. Fitted force-interval data at 100% Lmax showing the total curve and also the mathematically isolated alpha and beta processes.

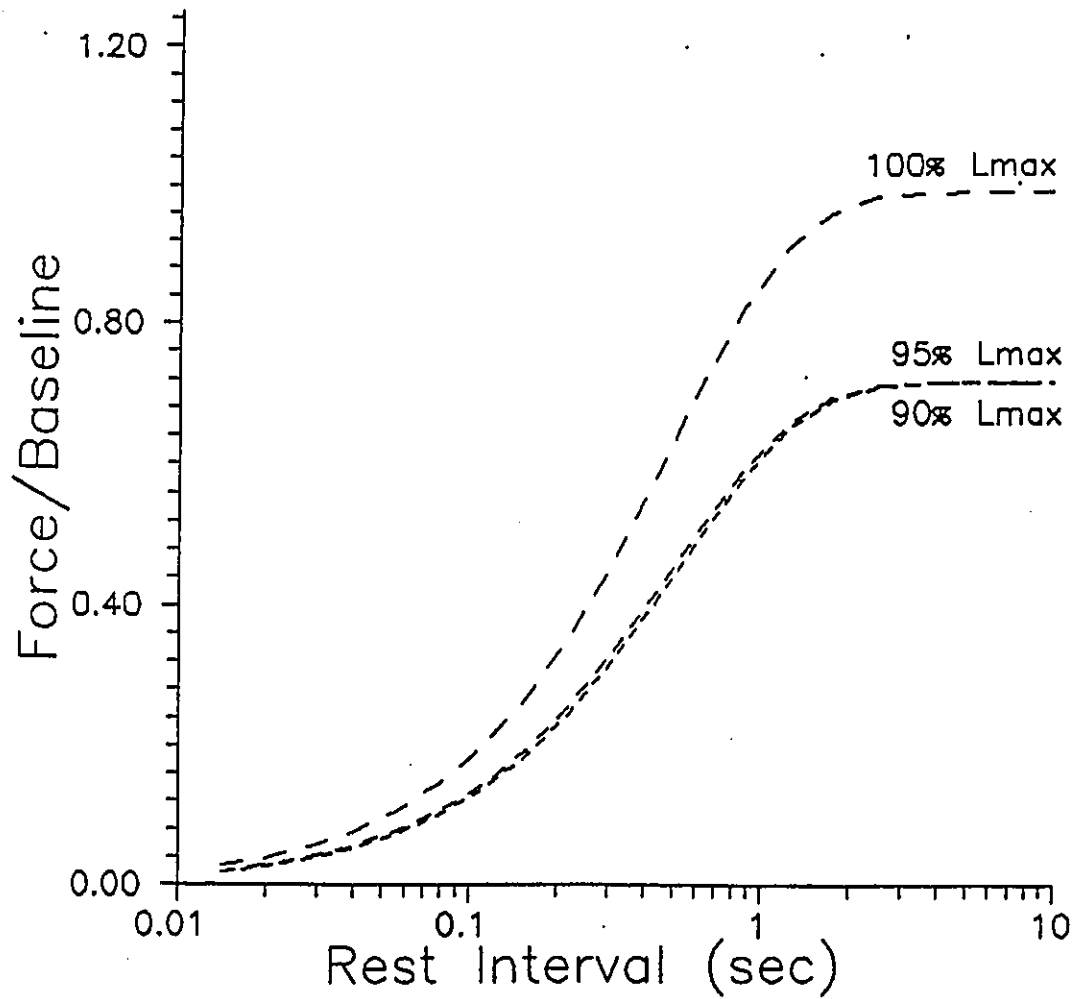


Figure 10. Mathematically isolated alpha processes overlayed from each of the three muscle lengths plotted on a logarithmic x-axis.

the data in Table 3 it can be seen that the percent contribution of the alpha process at L_{max} was 50% of the total curve. At 95 and 90% L_{max} the alpha contribution was dramatically reduced to 27% and 23% respectively, of the total curve.

Another quantitative measure used to characterize the alpha processes was the first time constant which reflects the time required to progress through 66.33% of the total curve. For all lengths studied, the first time constants for the alpha phase remained relatively unchanged at approximately 0.5 seconds.

The resting muscle length also had significant influence on the maximum rate of the alpha component. At L_{max} , there was a 16% greater increase in the maximum rate of the alpha phase compared to the shorter lengths.

The effect of resting muscle length on the beta process is shown in Figure 11. In contrast to the alpha process, the beta phase becomes more dominant as muscle length is reduced from L_{max} . Careful examination of Figure 11 shows that not only is the amplitude increased at shorter muscle lengths, but also there appears to be an earlier activation (leftward shift) of this process.

From Table 3 it is apparent that the percent contribution of the beta phase to the total curve was progressively increased as muscle length was reduced below optimum. Specifically, the contribution increased from 50% at L_{max} to a more dominant 73% and 77% at 95% and 90% L_{max}

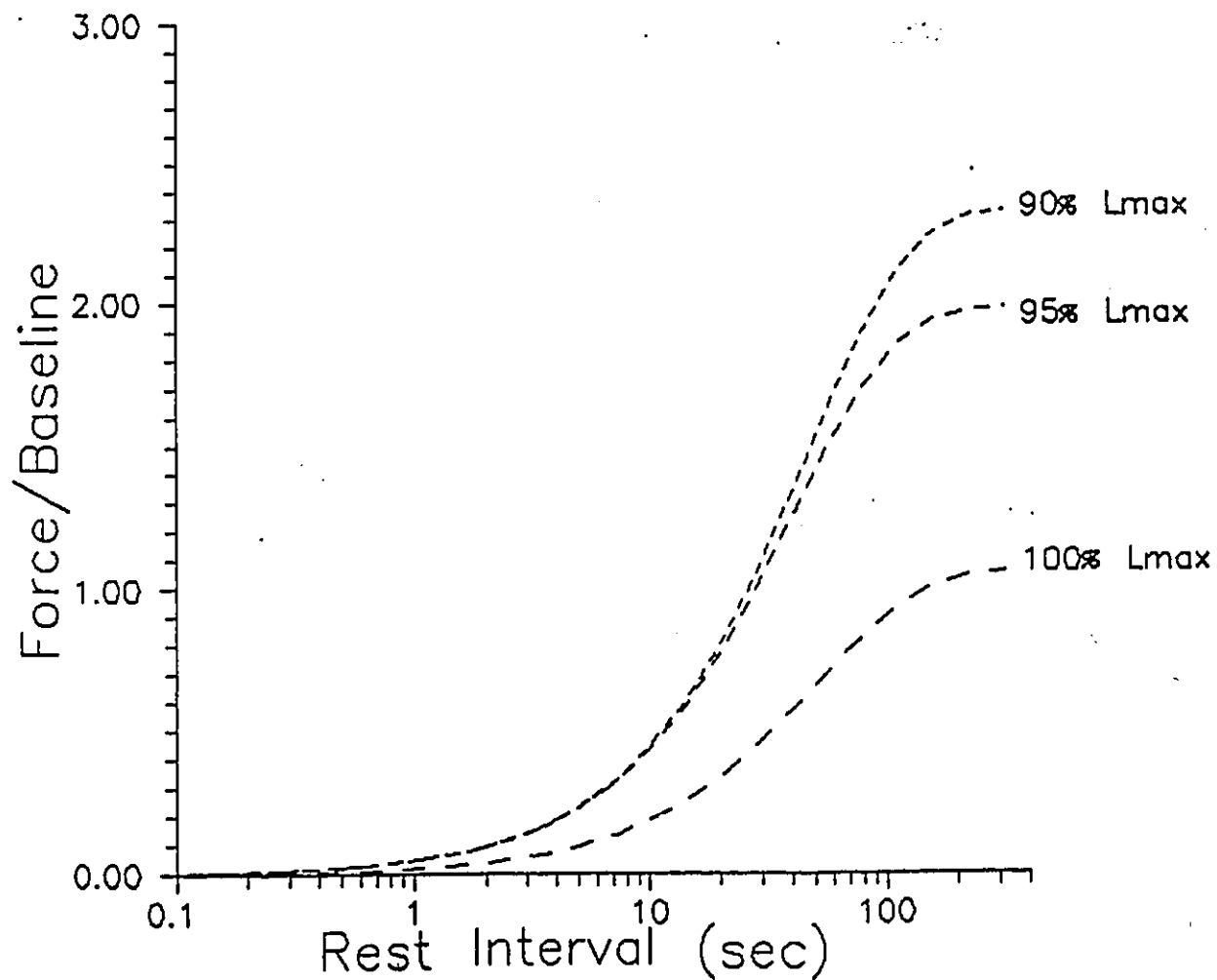


Figure 11. Mathematically isolated beta processes overlayed from each of the three muscle lengths and plotted on a logarithmic x-axis.

Table 3. The influence of resting muscle length on parameters used to characterize the force-interval relationship in right ventricular papillary muscle.

Muscle Length (% Lmax)	Max. Degree of Potentiation	Max. Rates (units/msec)		Contribution Alpha:Beta (%)	Time Constants	
		Alpha	Beta		Alpha	Beta
100	2.04	1873.9	13.3	50:50	0.50	51.15
95	2.68	1569.0	31.9	27:73	0.50	40.05
90	3.03	1564.3	39.5	23:77	0.52	46.94

respectively.

The first time constant of the beta phase also showed a dependence on muscle length. At L_{max} , the first time constant was 51.15 seconds and a reduction in muscle length to 95% of optimal length yielded a 22% reduction in the first time constant whereas only an 8% reduction, (relative to 100% L_{max}) in the time constant was found at 90%.

An examination of the maximum rates of the beta phases following a reduction in muscle length to 95% and 90% L_{max} demonstrated that the maximum rates increased by 239% and 297% respectively relative to L_{max} .

Potentiation decay

To determine whether the beat to beat loss of Ca^{++} from the cell was length-dependent, potentiation decay was examined at the three muscle lengths following a rest period of 121.0 seconds. This rest interval was chosen because it yields near maximal potentiation at all muscle lengths and this high degree of potentiation is critical for accurate determinations of the decay fraction or recirculation fraction (Schouten, 1985). Figure 12A shows an actual data file collected for a muscle at 100% L_{max} in 1mM Ca^{++} . The first two contractions represent the steady-state force development prior to the 121.0 second rest interval. The third contraction represents the potentiated beat following the rest interval with the subsequent beats reflecting the beat to beat decay of potentiation.

Assuming that the amount of Ca^{++} used by the muscle for subsequent contractions following the potentiated beat is constant ie. the recirculation fraction, (r in Figure 1), then the loss of force with each beat should reflect the fraction of Ca^{++} lost from the cell ($1-r$ in Figure 1.) from beat to beat (Morad and Goldman, 1973).

The data for each muscle length were linearized by plotting the force/baseline values for a given contraction as a function of the force/baseline value of the previous beat as shown in Figure 12B. Thus the recirculation fraction of Ca^{++} was derived from the slope of a linear best-fit line for 100, 95 and 90% L_{max} . Examination of

Figure 12. Panel A: an actual data file showing potentiation decay. Beats 1 and 2 represent the steady-state force development at a pacing frequency of 0.2Hz. Beat 3 represents the potentiated beat following a 121.0 second rest interval, while the remaining beats represent the decay of potentiation down to steady-state force development.

Panel B: Linearized potentiation decay plot at 100, 95 and 90% Lmax. The linear best fit lines yielded the following equations: at 100% Lmax $y = 0.627148x + 0.341027$; 95% Lmax $y = 0.556829x + 0.4164$; 90% Lmax $y = 0.547101x + 0.419147$.

F/B = force/baseline force development

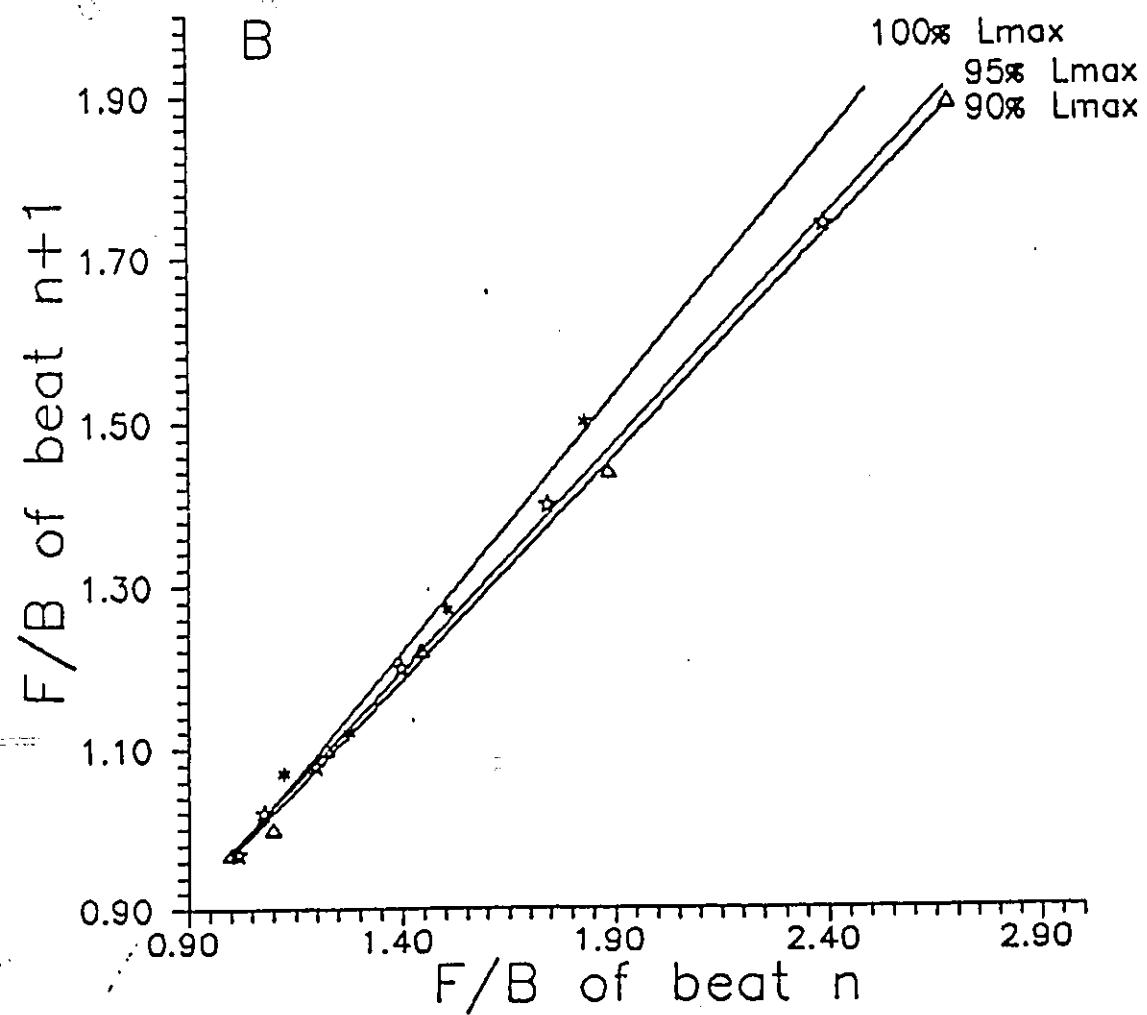
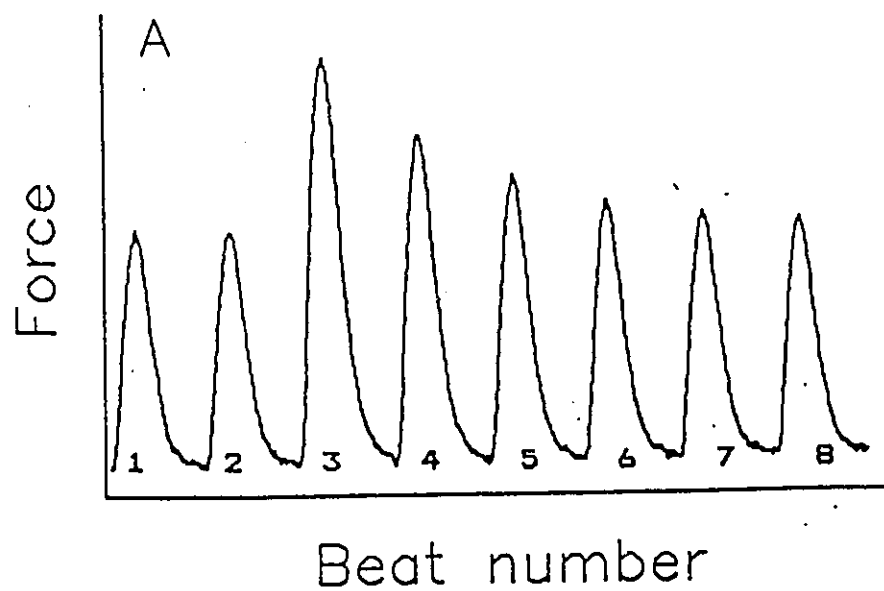


Figure 12B shows that the slopes become less steep as muscle length is reduced from optimal. This can be interpreted in two manners: 1. indicating that amount of Ca^{++} recirculated between contractions was progressively larger with increasing muscle length or, 2. conversely, that the fraction of Ca^{++} extruded from the cell between beats was progressively greater as muscle length was reduced from L_{max} . The linear best-fit method described above yielded a recirculation fraction of 63% at L_{max} and somewhat smaller fractions of 56% and 55% at 95 and 90% L_{max} respectively.

Buffer exchange experiments

To maximize any effect that muscle length may have on the $\text{Na}^+/\text{Ca}^{++}$ exchanger, only the extreme muscle lengths of 100 and 90% of L_{max} were utilized in the following experiments.

Figure 13 shows the effect of muscle length and extracellular Ca^{++} on the degree of rest potentiation following a 121.0 second rest interval. With an extracellular Ca^{++} concentration of 1.0mM, and the muscle at L_{max} , the degree of potentiation following the 121.0 second rest interval was 1.71. By reducing the muscle length to 90% L_{max} , the degree of potentiation increased to 3.03 indicating once again that force recovery was improved with a decrease in muscle length.

To determine the effect of a Ca^{++} reduction on the processes associated with rest potentiation and to determine whether this would be altered by the resting muscle length, an additional set of experiments were performed. A reduction in extracellular Ca^{++} caused a further improvement in potentiation at both lengths studied. A reduction to 0.5mM extracellular Ca^{++} revealed a comparable increase in the degree of potentiation, regardless of muscle length, from 1.71 to 3.22 at 100% L_{max} and from 3.03 to 4.62 at 90% L_{max} . The dashed lines drawn on this figure are simply straight lines drawn through the data points which give an indication of the change in the degree of potentiation as a result of the intervention.

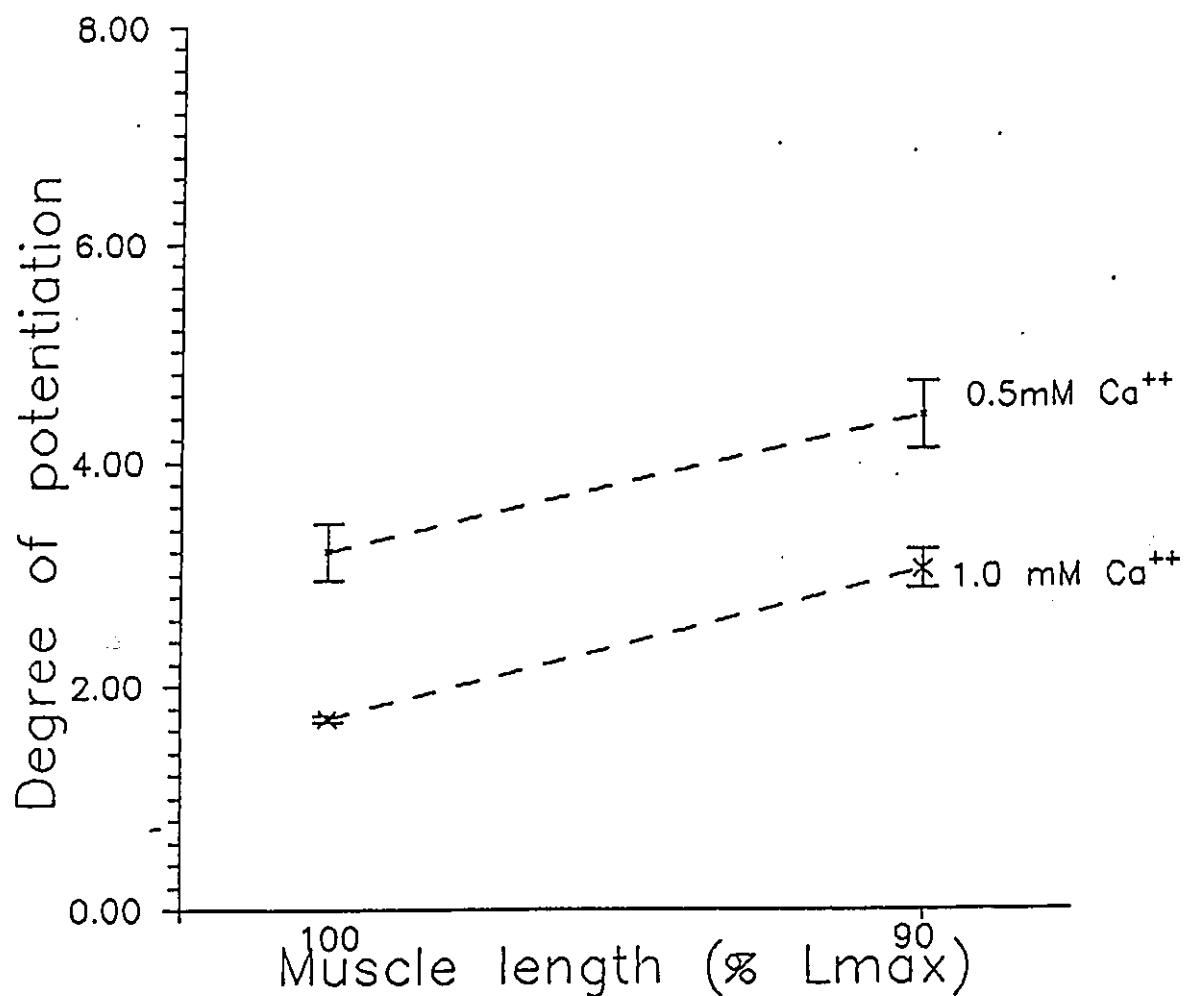
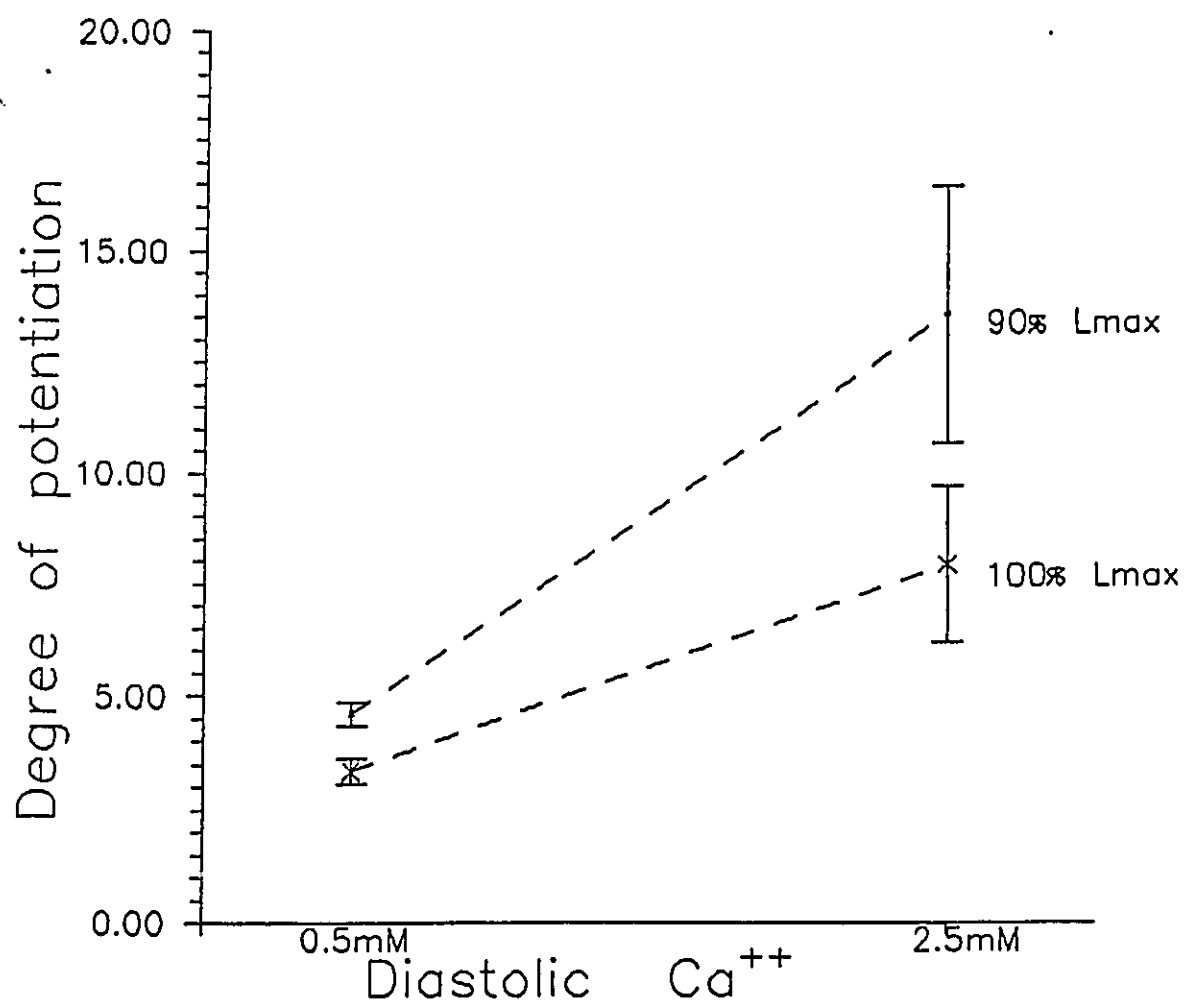


Figure 13. The effect of muscle length and Ca^{++} on rest potentiation in rat papillary muscle. The degree of potentiation following a 121.0 second rest interval was measured at 100% L_{max} and 90% L_{max} in both 1.0 mM and 0.5mM extracellular Ca^{++} . Values are mean \pm SEM, N=4-6 animals.

Given the fact that these lines are parallel, reinforces this observation that the degree of potentiation following the reduction in extracellular Ca^{++} was equally amplified at both lengths.

A series of fast flow buffer exchange experiments were then carried out in order to determine whether or not the activity of the exchange compartment, and more specifically the $\text{Na}^+/\text{Ca}^{++}$ exchanger, was dependent upon the resting muscle length. It was hypothesized that if the exchanger was responsible for the length-dependent alterations in the beta phase, then by subjecting the muscle, during the 121.0 second rest interval, to a new buffer whose composition was designed to specifically alter the activity of the exchanger, there should be a disproportionate change in the developed force due to a change in the myoplasmic Ca^{++} following the rest interval within each muscle length. In other words, when the inotropic state was altered by the fast flow buffer exchange, a reduction in muscle length would cause a greater relative increase in contractile force on the potentiated contraction. The results of experiments designed to test this hypothesis are shown in Figures 14 and 15.

Figure 14. The influence of muscle length and diastolic Ca^{++} on rest potentiation. Within each muscle length, 100 and 90% L_{max} , the muscles were perfused in 0.5mM Ca^{++} during the steady-state stimulation and were subsequently subjected to a rest interval of 121.0 second duration. During this interval, the muscles were either maintained in the 0.5mM Ca^{++} buffer or a quick exchange was performed to a buffer containing 2.5mM Ca^{++} . The force developed on the beat following the rest was plotted as a ratio of the steady-state force development. Values are means \pm SEM, N=4-6 animals



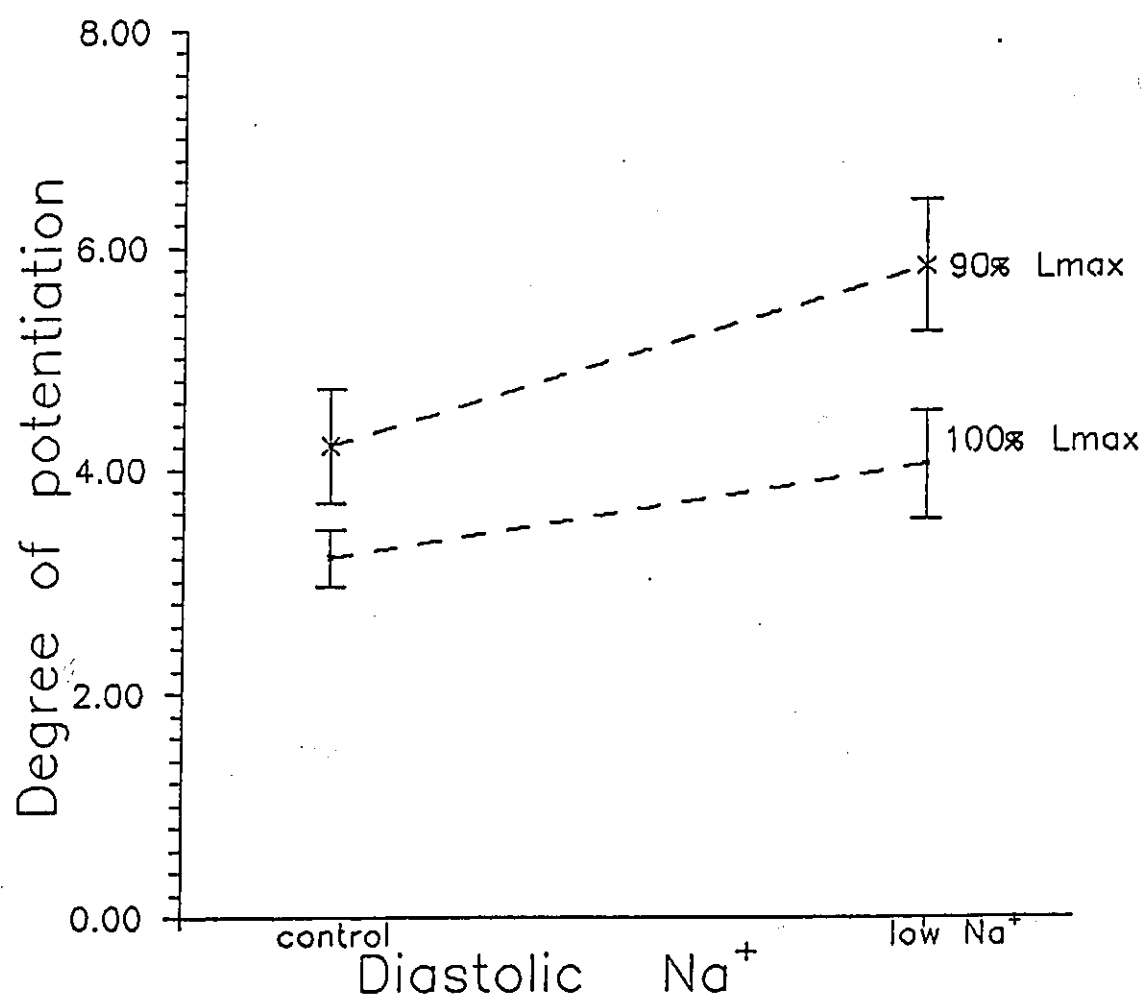
By subjecting the muscle to a high level of extracellular Ca^{++} during the 121.0 second rest interval, this set of experiments was designed to determine whether the influx of Ca^{++} through the $\text{Na}^+/\text{Ca}^{++}$ exchanger was dependent upon the resting muscle length. The muscles, perfused with 0.5mM Ca^{++} during steady-state stimulation, were subjected to a new buffer (via a quick-exchange) during the 121.0 second rest period containing 2.5mM Ca^{++} .

This reduction in extracellular Ca^{++} to 0.5mM to maximize the response was previously justified by the data in Figure 12. At L_{max} , the degree of potentiation following a 121.0 second rest interval increased from 3.22 in 0.5mM Ca^{++} to 7.94 following the buffer exchange to 2.5mM Ca^{++} (Figure 13). At 90% L_{max} , there was a disproportionate increase in the degree of potentiation following the buffer exchange relative to 100% as reflected by the different slopes of the dashed lines. Specifically, the degree of potentiation increased from 4.61 to 13.54 when subjected to the higher Ca^{++} load at the shorter muscle length.

The second intervention used to specifically alter the activity of the $\text{Na}^+/\text{Ca}^{++}$ exchanger was to subject the muscle to a 40% reduction in extracellular Na^+ (70.26mM) during the 121.0 second rest interval. These results are shown in Figure 15.

When subjected to the rest period under control conditions (ie. 117.1mM NaCl) the muscles potentiated to an average of 3.21 and 4.21 at 100% and 90% L_{max} respectively.

Figure 15. The influence of muscle length and diastolic Na^+ on rest potentiation. Within each muscle length, 100 and 90% L_{max} , the muscles were perfused in 0.5mM Ca^{++} and 117.1mM Na^+ during the steady-state stimulation and were subsequently subjected to a rest interval of 121.0 second duration. During this interval, the muscles were either maintained in the 0.5mM Ca^{++} ; 117.1mM Na^+ buffer or a quick exchange was performed to a buffer containing 70.26mM Na^+ . The force developed on the beat following the rest was plotted as a ratio of the steady-state force development. Values are means \pm SEM. N=4-5 animals.



By substituting the low Na^+ buffer via a quick exchange, there was, once again, a disproportionate increase in the degree of potentiation following the rest interval. At L_{max} , the potentiation increased from 3.21 to 4.02, as a result of exposure to the 40% reduction in Na^+ during the 121.0 second rest period. At the shorter length, the effect of the low Na^+ was more pronounced yielding an increase from 4.21 under control conditions to 5.79 in the low Na^+ .

DISCUSSION

Twitch characteristics

The ability of muscle length to modulate force development has been well established since the early studies of Frank and Starling. With isolated cardiac muscle, a small change in the resting muscle length causes a relatively large change in the force developed during the contraction. As length is increased, the force of contraction rises steeply, in a curvilinear manner, to a point of maximal force development, defined as L_{max} , (Tortora and Evans, 1986; ter Keurs et al., 1980b; Wohlfart et al., 1977).

A cellular mechanism to explain this effect of muscle stretch on myocardial performance has been the focus of considerable study (Babu et al., 1988; Hoffman and Fuchs, 1987, 1988; Kentish et al., 1986). Given the crucial role of Ca^{++} in the regulation of activation/contraction, length-dependent alterations in Ca^{++} handling at the cellular level have been implicated as possible mechanisms to explain the length-dependent modulation of twitch force.

Basic twitch characteristics can yield valuable information regarding the movement of Ca^{++} during a single instantaneous contraction. It should be recognized that while the twitch characteristics themselves cannot reveal specific mechanisms, they do allow for inferences or speculation regarding the mechanisms of E-C coupling as

they are expressed through the processes of contraction and relaxation. The determination of the specific mechanisms underlying the alterations in the basic twitch parameters would require additional experimental techniques that are beyond the scope of this study.

The majority of studies however have simply used the force parameters of the twitch function curve as a verification of a cardiomyopathic state (Fein et al., 1980; Pogessi et al., 1987) or as an index of a drug effect (Pogessi et al., 1982). To my knowledge, only minimal information presently exists regarding the influence of muscle length on the various parameters used to characterize a muscle twitch (Pogessi et al., 1984; Allen and Kurihara, 1982).

In the generation of the length-tension relationship, peak force is measured at a variety of muscle lengths corresponding to a given percentage of L_{max} . In addition to analyzing the amplitude of the twitch, the shape of the curve can also provide information regarding the processes involved in attaining the maximal amplitude and returning from the peak contractile response. Thus a complete analysis of a single twitch should involve not only force indices such as peak force and the maximum positive and negative rates of force development, but also the various timing characteristics associated with the function curve.

In this study, I have extensively characterized a single muscle twitch in terms of both force and timing

parameters. The present results not only support previous investigations (Allen and Kurihara, 1982; Pogessi et al., 1984; Kentish et al., 1986; Taylor et al., 1989) but also extended the knowledge regarding the influence of muscle length on twitch function.

As expected from the length-tension relationship, the peak contractile force was positively related to the extent of muscle stretch (Table 1). Traditionally, this response was attributed to purely physical factors such as an increase in the number of cross-bridge formations between the contractile proteins, actin and myosin, as the muscle length was increased to L_{max} .

If the degree of myofilament overlap were the sole reason for the increase in force, with no change in the inotropic state, it would follow that while the peak force should be increased with stretch, the shape of the twitch function curve should only differ in its amplitude. In other words, the curves should be superimposable indicating that the processes of contractile activation such as Ca^{++} release from the SR, and the myofilament Ca^{++} binding remain constant regardless of muscle length. More recently it has been shown in both isolated tissue (Allen et al., 1974; Fabiato, 1975; Kentish et al., 1986; Allen and Kurihara, 1982) and whole heart (Stefanon et al., 1990) preparations that these activation processes are, in fact, modulated by the resting muscle length.

The analysis of the twitch characteristics in the

present study have provided additional evidence that purely physical factors alone cannot explain the length-dependent force production. In addition to altering the number of cross-bridge formations, muscle length has indeed affected the activation level of the cell.

The reduction in the maximum rates for both relaxation and contraction at the shorter muscle lengths (Table 1) are consistent with the idea that the processes associated with the activation/deactivation of the cardiac cell are dependent upon the length of the muscle. Specifically, these may indicate that either the amount of Ca^{++} released to the myofilaments (Fabiato and Fabiato, 1975; Fabiato 1980; Lakatta and Lappe, 1981) and/or the sensitivity of the myofilaments (Hoffman and Fuchs, 1987; Allen and Kurihara, 1982) was increased with increasing muscle length. These mechanisms could explain the changes in the slope of the curve during both the contraction and relaxation phases.

If there exists a coupling between the processes of contraction and relaxation, then the ratio of both the positive and negative maximum rates will provide information as to whether or not the muscle length has a uniform effect on these cellular processes associated with E-C coupling. The progressive reduction in this ratio with decreasing muscle length found in the present study (Table 1) suggests that muscle length uncoupled this relationship and has differentially affected one or both of these

processes. This could result from a number of combinations of increases and decreases in the positive or negative rates, however, at this point, the specific manner by which this uncoupling may have occurred cannot be determined.

Evidence to suggest that the processes associated with relaxation are length-dependent was determined in the present study. It has been established that the Ca^{++} transient reaches a peak at or near the point of maximal rate of positive force development (Yue, 1987; Orchard and Lakatta, 1985; Allen and Kurihara, 1982). Therefore, the similar percent reductions in the timing parameters between the maximal rate of force development (T1) and complete relaxation (T4) inclusively, as muscle length is reduced from 100 to 90% L_{max} (Table 2) would suggest that the processes associated with the decrease of the Ca^{++} transient are length-dependent.

The present finding that the time required to achieve maximal rate of force development was not altered by the resting muscle length (Table 2) would suggest that the processes associated with the rise of the Ca^{++} transient may not be length-dependent. Indeed, Allen and Kurihara (1982) have shown that when superimposed, the rise of the Ca^{++} transient was unchanged at the long or short muscle lengths while the time course of the fall of the transient was abbreviated at the longer muscle length.

If the Ca^{++} binding affinity of troponin is greater at the longer muscle lengths, then it would be expected that

the dissociation of Ca^{++} from troponin would occur more slowly at the longer lengths and in turn prolong the relaxation times (Allen and Kurihara 1982; Kentish et al., 1986) and vice versa. In the present study, the progressive reduction in time to complete relaxation with decreasing muscle length are consistent with the idea that binding of Ca^{++} to troponin is affected by a change in the resting muscle length.

Force-interval experiments

With increasing duration of a diastolic interval, rat papillary muscle exhibits a phenomena of rest potentiation (Shattock and Bers, 1989; Arlock et al., 1988) which is in contrast to many other species that exhibit a characteristic rest decay when subjected to long diastolic intervals (Cooper and Fry, 1990; Arlock et al., 1988; Liu et al., 1988; Janczewski et al., 1988). This response in the rat has also been shown to involve two processes that contribute to the overall ability of the muscle to recover force between beats (Johannsson and Asgrimsson, 1988; Cooper and Fry, 1988; Arlock et al., 1988; ter Keurs et al., 1987). The initial phase is very rapid followed by a more slowly acting second phase (Johannsson and Asgrimsson, 1988; Bottinelli et al., 1988).

These facts imply that for the rat, the processes associated with force recovery, occur over a much longer

period of time compared to other mammalian species (Johannsson and Asgrimsson, 1988). Thus, the studies which have utilized a relatively rapid steady-state stimulation pattern to examine the effect of muscle length on excitation-contraction coupling in the rat have interrupted these processes of force recovery between beats and have therefore not allowed them to evolve and express their maximal capability.

The force-interval relationship reflects the dynamic movements of Ca^{++} as these processes evolve through time. This allows for the examination of the underlying cellular processes which otherwise are difficult or impossible to examine directly.

A recent model of excitation-contraction coupling has been developed to describe the force-interval relationship in rat ventricular muscle (Schouten et al., 1987). This model includes the conventional uptake and release sites for Ca^{++} and was extended to include an exchange compartment in order to explain the late development of maximum force at approximately 100 seconds of diastolic rest (Schouten, 1985).

While Johnson (1979) has reported that the short-term force-interval relationship lacked a dependence upon muscle length when the maximum rate of tension development was used as the contractile index, My research has found a number of length-dependent alterations in the force-interval relationship using muscle lengths corresponding to

100, 95 and 90% L_{max}. These muscle lengths were selected because they cover a wide range of the ascending limb of the length-tension relationship (Allen et al, 1974; Anderson et al., 1977).

It has been well established that muscle length has a direct effect on the Ca^{++} binding affinity of troponin and therefore, during the examination of the twitch characteristics, plays a major role in the response of the muscle. On the other hand, the force-interval data was collected to ensure that any change in the myofilament Ca^{++} sensitivity with a change in muscle length would not confound the results.

Given that muscle length was held constant throughout the entire force-interval data collection within each muscle length, any alterations found would be independent of changes in myofilament Ca^{++} sensitivity and solely reflect a length-dependence of the processes associated with the force recovery between beats.

Because the force-interval response of cardiac muscle in the present study is modelled for two simultaneous and independent processes, the alterations may arise from independent effects on either or both of these processes rather than simply an amplification or depression in the total response.

In terms of the force-interval curve, it is evident from Figure 8 that muscle length had opposing effects on the alpha and beta processes. Specifically, the

alpha process was more dominant at L_{max} , while shorter muscle lengths favoured the beta phase. From this one may speculate that the functioning of the SR is improved with increasing stretch up to L_{max} , which is supported by Fabiato (1975), and conversely, that the Ca^{++} handling ability of the SL may be improved during long rest periods at shorter muscle lengths when the SR function may be depressed. Because biochemical studies cannot determine the effect of muscle length on the functioning of either the SL or SR Ca^{++} pumps, one can only speculate or infer changes based upon their physiological function.

The rightward shift and depression in the alpha phase of the force-interval relationship found with decreasing muscle length (Figure 10) lends further support for a length-dependent functioning of the SR. Given that the alpha process reflects the uptake of Ca^{++} from the myoplasm, its transfer to the release compartment and its subsequent release following excitation, this result suggests that one or more of these processes are length-dependent. The rightward shift of the alpha phase with decreasing muscle length suggests that this process has become less sensitive or perhaps inhibited at the shorter muscle lengths. However, further studies, which are beyond the scope of this thesis, are required to specifically determine which of these processes are altered by muscle length.

In terms of the beta phase, the progressively higher

potentiation with decreasing muscle lengths (Figure 7) is similar to that found by Pogessi et. al., (1984). If one assumes that 1) the sensitivity of the myofilaments increases with increasing muscle length (Hoffman and Fuchs, 1987; Kentish et al., 1986) and 2) that the amount of Ca^{++} released is progressively reduced at muscle lengths less than L_{max} (Fabiato, 1975), then the present findings might suggest that a negative feedback system exists between these two processes of intracellular Ca^{++} handling.

At longer muscle lengths the myofilaments are more sensitive to Ca^{++} and therefore may require less Ca^{++} to be released following excitation to produce a given level of force. On the other hand, when muscle length is shortened, the myofilament sensitivity to Ca^{++} is reduced and, therefore, must be compensated for by mechanisms that increase myoplasmic Ca^{++} availability. It should be noted however, that while the potentiation was increased at shorter muscle lengths, the absolute levels of force development remained smaller relative to L_{max} .

At L_{max} , a number of studies have shown that the alpha and beta processes, under control conditions, each contribute an equal percentage of about 50% to the total force-interval curve (Taylor et al., 1989; McComb, 1990; Gamble, 1990).

The large increase in the percent contribution of the beta phase, and decrease in the alpha contribution, with decreasing length (Table 3) would also suggest that the

coupling of these alpha and beta processes has been disrupted by an reduction in muscle length. Similar disruptions in this interaction of the alpha and beta processes have been found with diabetic (McComb, 1990) and hypertrophic (Taylor et al., 1989) models and have been attributed to a possible alteration in the activity of the exchange compartment.

Buffer exchange experiments

Similar to the present study, Pogessi et al., (1984), using post-extrasystolic potentiation (PESP), have demonstrated that at muscle lengths shorter than L_{max} , the degree of potentiation increased on the beat immediately following an extrasystole. They concluded that one or more of the Ca^{++} handling processes were length-dependent but could not identify a possible mechanism by which this increase in potentiation may have occurred.

With the current model of E-C coupling, it has been suggested that the late maximum of force development (potentiation) found in the rat heart is a result of additional accumulation of Ca^{++} from an exchange compartment located at the sarcolemma (Schouten, 1985). The activity of this exchange compartment is thought to be regulated by the activity of the Na^{+}/Ca^{++} exchanger and the Na^{+}/K^{+} ATPase pump (Schouten et al., 1987; ter Keurs et al. 1987).

The increase in potentiation found during the beta phase at shorter muscle lengths (Figure 11) could result from either an increased influx of Ca^{++} or a reduction in the amount of Ca^{++} extruded from the cell, via the $\text{Na}^+/\text{Ca}^{++}$ exchanger, during periods of rest. In order to determine which of these may be responsible for the present results, it is necessary to determine the functional mode of the $\text{Na}^+/\text{Ca}^{++}$ exchange mechanism itself.

The $\text{Na}^+/\text{Ca}^{++}$ exchanger has traditionally been considered to act as an effluxer for Ca^{++} (forward mode) during steady-state stimulation where Ca^{++} is extruded from the cell in exchange for Na^+ entering the cell down its electrochemical gradient (Reugg, 1986). Sutko et al., (1986) however, have argued that an increase in the level of rest potentiation is not likely to result from a depressed Ca^{++} efflux since the extrusion of Ca^{++} via the exchanger is depolarization dependent.

Shattock and Bers (1989), examining the phenomena of rest potentiation in the rat have recently demonstrated a loss of extracellular Ca^{++} during a 30 second period of rest with a concomitant increase in the levels of extracellular Na^+ . They concluded that there was a net cellular Ca^{++} gain due to the transfer of extracellular Ca^{++} to the intracellular space via the $\text{Na}^+/\text{Ca}^{++}$ exchanger (reverse mode). Indeed, the high Na^+ activity that also exists in the rat cardiac muscle would tend to thermodynamically favour Ca^{++} entry through the $\text{Na}^+/\text{Ca}^{++}$

exchanger at the resting membrane potential (Bers et al., 1990; Shattock and Bers, 1989).

This is consistent with the notion that in the rat, the operational mode of the exchanger during diastolic rest periods is as an influxer for Ca^{++} (Janczewski and Lewartowski, 1986; Bers, 1985) which is indeed proposed by the most recently developed model of E-C coupling (Schouten et al. 1987; Taylor et al., 1989; Schouten, 1985).

One problem in determining the physiological role of the $\text{Na}^+/\text{Ca}^{++}$ exchanger is the lack of any specific inhibitors. While various amiloride derivatives have been recently used in an attempt to reduce the $\text{Na}^+/\text{Ca}^{++}$ exchanger activity, (Pierce et al., 1990; Siegl et al., 1984) they are known to have fairly widespread effects on other cellular systems (Bers et al., 1988).

The electrogenic nature of the $\text{Na}^+/\text{Ca}^{++}$ exchanger would suggest that alterations in the ionic environment would not only have a direct effect on its activity level but also on its functional mode.

In the present study it was hypothesized that the $\text{Na}^+/\text{Ca}^{++}$ exchanger was responsible for the increased potentiation found at muscle lengths less than L_{max} . In order to test this hypothesis, the extracellular environment was altered at 100 and 90% L_{max} to specifically alter the activity of the exchanger. Only these two extreme muscle lengths were used in order to maximize the response of the muscle during the buffer exchanges. If the activity of the exchanger is dependent upon the muscle length, then

at the different level of inotropic state there should be a disproportionate change in potentiation between the two muscle lengths.

A reduction in extracellular Ca^{++} from 1.0mM to 0.5mM was found to increase the degree of potentiation at both 100 and 90% L_{max} (Figure 13). The fact that a decrease in the extracellular Ca^{++} caused an equivalent increase in the degree of potentiation at both muscle lengths suggests that, when equilibrated at the reduced Ca^{++} level, there was no net effect of muscle length on the processes occurring between beats. In other words, the degree of potentiation following the rest interval at 100% L_{max} was simply amplified at the shorter muscle length.

Having determined that there was no net length effect when the extracellular Ca^{++} concentration was reduced, I was therefore able to reduce the steady-state $[\text{Ca}^{++}]$ to 0.5mM during the fast-flow buffer exchange experiments in order to maximize any experimental effects and eliminate any confounding variables in terms of a length effect during steady-state stimulation.

During steady-state stimulation, this reduction in extracellular $[\text{Ca}^{++}]$ reduced the developed force by approximately 50% (not shown). This reduction in steady-state force development may be increasing the muscle's capacity to accumulate further Ca^{++} during periods of rest and therefore increase the degree of rest potentiation.

It is interesting that, regardless of muscle length,

the degree of potentiation following the 121 second rest interval was further increased in 0.5mM Ca^{++} versus 1.0mM Ca^{++} (Figure 13). At this point, I have no reasonable explanation for this result. This finding might be expected if it is assumed that, even in 1.0mM Ca^{++} , one or more of the Ca^{++} handling processes associated with force recovery between beats was/were saturated. This is only speculative and requires further investigation to obtain direct evidence for this hypothesis.

In order to determine whether or not the muscle length modulated the activity of the $\text{Na}^{+}/\text{Ca}^{++}$ exchanger, the muscles were subjected to two ionic modifications during the 121 second rest interval. These modifications were designed to specifically alter the activity of the exchanger itself. These included 1) a five fold increase in the extracellular $[\text{Ca}^{++}]$ and 2) a 40% reduction in the extracellular $[\text{Na}^{+}]$. These results are shown in Figures 14 and 15 can be interpreted in the following manner.

By exposing the muscle to a high level of extracellular Ca^{++} during the rest interval, when the exchanger was acting in an influxing mode (Shattock and Bers, 1989; Janczewski and Lewartowski, 1986) the driving force for Ca^{++} into the cell was enhanced so that the SR could accumulate more Ca^{++} and the force on the subsequent beat was increased (Bers, 1985). This increase in potentiation was found to be disproportionate between the two lengths and is consistent with the view that the length

modulates this accumulation of Ca^{++} into the cell via the $\text{Na}^+/\text{Ca}^{++}$ exchanger. It is not likely that the Ca^{++} channels contributed to the influx of Ca^{++} given that they are considered to be voltage dependent (Reugg, 1986).

The 40% reduction in the extracellular $[\text{Na}^+]$ was used, in this study, to reduce the Na^+ gradient across the sarcolemma which should inhibit the activity of the $\text{Na}^+/\text{Ca}^{++}$ exchanger (Sonn and Lee, 1988) regardless of whether it is acting in the forward (efflux) or reverse (influx) mode.

In addition to reducing the Na^+ gradient across the sarcolemma (Bers, 1987), a reduction in $[\text{Na}^+]_o$ has been shown, during steady-state stimulation, to increase the force of contraction (Bers, 1987; Sonn and Lee, 1988), reduce the resting membrane potential (V_m) and diminish the intracellular Na^+ activity ($a_{\text{Na}^+}^i$) (Sonn and Lee, 1988).

Shattock and Bers (1989) have shown that, during diastole, the extracellular Ca^{++} decreases and have attributed it to an influx of Ca^{++} via the $\text{Na}^+/\text{Ca}^{++}$ exchanger, this response was not instantaneous and evolved with time during the diastolic period. They reported that during the initial stage of the diastolic period, the extracellular Ca^{++} remained elevated suggesting that the exchanger was acting in the forward mode (ie. efflux). As the duration of this rest progressed, there was an apparent transient reversal of the mode of the exchanger to an influx for Ca^{++} . The time course for this reversal in the

operational mode of the exchanger from a Ca^{++} effluxer to an influxer however, cannot be directly determined from their results but appears to have occurred at approximately 15 seconds into the rest interval.

Therefore, the present finding that a 40% reduction in extracellular Na^+ during diastole potentiated the muscle at both 90 and 100% L_{max} but to a lesser degree than with the Ca^{++} exchange experiments, suggests that the reduction in extracellular Na^+ has affected the activity of the $\text{Na}^+/\text{Ca}^{++}$ exchanger in both the forward and reverse mode.

Early during the diastolic period the efflux of Ca^{++} through the $\text{Na}^+/\text{Ca}^{++}$ exchanger would have been inhibited resulting in a net accumulation of cellular Ca^{++} which would be sequestered by the SR. With the more prolonged period of rest, when it is assumed that Ca^{++} would be entering the cell through the exchanger, the inhibition of this process would reduce the influx of Ca^{++} thereby limiting the SR Ca^{++} accumulation and resulting in a depressed degree of potentiation.

The difference in the degree of potentiation between the two exchange experiments may have arisen due to the fact that the driving force for Ca^{++} into the cell may have been greater during the high Ca^{++} condition as compared to the low Na^{++} condition.

The disproportionate changes in the degree of potentiation between the two muscle lengths, when subjected to the fast-flow buffer exchange, would suggest that the

muscle response was modulated by the resting muscle length. Given that fact that the exchanger was the only means by which the cells could have accumulated Ca^{++} , then it must be concluded that the activity of the $\text{Na}^+/\text{Ca}^{++}$ exchanger was altered by changes in the resting muscle length.

Potential decay and the recirculation fraction of Ca^{++}

While my examination of the force-interval relationship did reveal length-dependent alterations in the force generation processes (alpha and beta), an analysis of potential decay would determine whether the Ca^{++} removal by the SR and/or SL were also length-dependent.

The decay of the force signal from a potentiated state provides a physiological means by which the fraction of Ca^{++} recirculated between the contractile proteins and the SR can be estimated (Ragnarsdottir et al., 1982; Morad and Goldman, 1973). The precision of this measurement is dependent on a high degree of potentiation and is a function of the number of beats following the potentiated state (Schouten, 1985). Therefore, to achieve a high level of potentiation, this study utilized a rest interval of 121.0 seconds which allowed a minimum of five beats following potentiation to be used for estimation of the recirculation fraction.

In the present study, I was able to verify the studies of Pogessi et al., (1984) and Taylor (personal communication) and have shown that muscle length does

effect the recirculation fraction of Ca^{++} . Therefore the Ca^{++} handling properties associated with the beat to beat loss of Ca^{++} from the cell, and in turn the beat to beat recirculation of Ca^{++} between the SR and the myofilaments are length-dependent. This increase in the recirculation fraction at the longer muscle lengths is consistent with the increased alpha phase found at L_{max} in the present study (Figure 8). These results are in agreement with Schouten et al.'s, (1987), proposing that the recirculation of Ca^{++} from the myofilaments to the uptake compartment (Figure 1) was a significant contributor to the force development during the alpha phase of force recovery. The specific manner by which this may occur requires further investigation.

SUMMARY AND CONCLUSIONS

The ability of stretch on the myocardium to modulate contractile force has now been well established. In order to provide a cellular explanation for what is now known as Starling's Law many studies have focussed on length-dependent alterations in the Ca^{++} handling ability of the cardiac cell. The majority of these studies are, by their design, considered to non-physiological.

The force-interval relationship allows one to examine the dynamic movements of Ca^{++} between contractions in a physiological preparation. Coupled with a mathematical model of E-C coupling, this method provided a means of quantifying the effect of muscle length on force recovery.

This study initially verified and extended the knowledge of the effect of muscle length on the basic twitch parameters used to characterize a single twitch.

Using the force-interval relationship, it was found that the alpha process was depressed at muscle lengths below optimum. The beta process, on the other hand, was progressively improved as muscle length was reduced from 100% through 95 and 90% L_{max} . Specifically, a 10% percent reduction in muscle length from L_{max} yielded a 50% increase in the degree of potentiation relative to L_{max} .

In order to determine a possible mechanism by which this increase in the beta phase may have occurred, a fast-flow buffer exchange technique was used to alter the inotropic level of the cells during rest and the

contractile force on the potentiated beat was measured. The disproportionate increase found between muscle lengths when both extracellular Na^+ and Ca^{++} were independently manipulated suggested that the muscle length does regulate the activity of the $\text{Na}^+/\text{Ca}^{++}$ exchanger.

To determine whether the efflux of Ca^{++} from the cell, and in turn the recirculation fraction of Ca^{++} was modulated by muscle length, the decay of force from a potentiated state was performed at different muscle lengths. Once again, muscle length was found to regulate the various processes associated with the beat to beat regulation of Ca^{++} .

Twitch characteristic data was also collected and exhibited a dependence upon muscle length. A number of both force and timing parameters used to characterize a single twitch were found to be significantly reduced at muscle lengths shorter than L_{max} .

In conclusion, this study has shown that intracellular Ca^{++} handling processes associated with force recovery between beats are dependent upon the resting muscle length. It therefore provides the basis for a number of studies attempting to examine physiological lesions in the Ca^{++} handling properties of the cardiac cell under conditions where the structural integrity of the myocardium has been altered thus limiting or enhancing its contractile function.

BIBLIOGRAPHY

- Allen, D.G., B.R. Jewell, and J.W. Murray (1974), The contribution of activation processes to the length-tension relation of cardiac muscle. Nature, 248:606-607.
- Allen, D.G., and S. Kurihara (1982), The effects of muscle length on intracellular calcium transients in mammalian cardiac muscle. J. Physiol., 327:79-94.
- Anderson, P.A.W., A. Manring and E.A. Johnson (1977), The force of contraction of isolated papillary muscle: a study of the interaction of its determining factors. J. Mol. Cell. Cardiol., 9:131-150.
- Arlock, P., B. Liu, B. Wohlfart, and B.W. Johansson (1988), A comparison of some force-interval relations in rat, hedgehog, and human cardiac preparations [abstract]. Cardiovasc. Res., 22:601.
- Babu, A., E. Sonnenblik, and J. Gulati (1988), Molecular basis for the influence of muscle length on myocardial performance. Science, 240:74-76.
- Bers, D.M. (1987), Mechanisms contributing to the cardiac inotropic effect of Na pump inhibition and reduction of extracellular Na. J. Gen. Physiol., 90:479-504.
- Bers, D.M. (1985), Ca influx and SR Ca release in cardiac muscle activation during postrest recovery. Am. J. Physiol., 248: H366-H381.
- Bers, D.M., D.M. Christensen, and T.X. Nguyen (1988), Can calcium entry via Na-Ca exchange directly activate cardiac muscle contraction? J. Mol. Cell. Cardiol., 20:405-414.
- Bers, D.M., W.J. Lederer, and J.R. Berlin (1990), Intracellular Ca transients in rat cardiac myocytes: role of Na-Ca exchange in excitation-contraction coupling. Am. J. Physiol., 258:C944-C954.
- Bottinelli, R., C. Pogessi, B. Polla, and C. Reggiani (1988), Effects of thyroid state and beta adrenergic stimulation on mechanical restitution of rat ventricular myocardium [abstract]. Cardiovasc. Res., 22:597.
- Bouchard, R.A., and D. Bose (1989), Analysis of the interval-force relationship in rat and canine ventricular myocardium. Am. J. Physiol., 257:H2036-H2047.
- Cooper, I.C., and C.H. Fry (1988), Mechanical restitution of isolated human myocardium is described by two exponential recovery processes [abstract]. Cardiovasc.

Res., 22:596.

Cooper, I.C., and C.H. Fry (1990), Mechanical restitution in isolated mammalian myocardium: Species differences and underlying mechanisms. J. Mol. Cell. Cardiol., 22:439-452.

Fabiato, A., and F. Fabiato (1975), Dependence of the contractile activation of skinned cardiac cells on the sarcomere length. Nature, 256:54-56.

Fabiato, A. (1980), Sarcomere length dependence of calcium release from the sarcoplasmic reticulum of skinned cardiac cells demonstrated by differential microspectrophotometry with Arsenazo III [abstract] J. Gen. Physiol., 76:15a.

Fein, F.S., L.B. Kornstein, J.E. Strobeck, J.M. Capasso, and E.H. Sonnenblik (1980), Altered myocardial mechanics in diabetic rats. Circ. Res., 47:922-933.

Forester, G. V., and G.W. Mainwood (1974), Interval dependent inotropic effects in the rat myocardium and the effect of calcium. Pfluegers Arch., 352:189-196.

Gamble, J. (1990), The effect of resting muscle length on the force-interval relationship in rat ventricular muscle. Independent study, University of Windsor.

Gordon, A.M. and G.H. Pollack (1980), Effects of calcium on the sarcomere length-tension relation in rat cardiac muscle: implications for the Frank-Starling Mechanism. Circ. Res., 47:610-619.

Hibberd, M.G., and B.R. Jewell (1982), Calcium and length-dependent force production in rat ventricular muscle. J. Physiol., 329:527-540.

Hoffman, P.A., and F. Fuchs (1987), Effect of length and cross-bridge attachment on Ca^{++} binding to cardiac troponin C. Am. J. Physiol., 253:C90-C96.

Hoffman, P.A., and F. Fuchs (1988), Bound calcium and force development in skinned cardiac muscle bundles: effect of sarcomere length. J. Mol. Cell. Cardiol., 20:667-677.

Janczewski, A., and B. Lewartowski (1986), The effect of prolonged rest on calcium exchange and contractions in rat and guinea-pig ventricular myocardium. J. Mol. Cell. Cardiol., 18:1233-1242.

Janczewski, A., B. Lewartowski, B. Pytowski and A. Prokopczuk (1988), Calcium exchange and force-interval relations [abstract]. Cardiovasc. Res., 22:591.

- Jewell, B.R. (1977), A reexamination of the influence of muscle length on myocardial performance. Circ. Res., 40:221-231.
- Johannsson, M., and H. Asgrimsson (1988), Mechanical restitution and post-extracontraction potentiation in guinea pig and rat atria [abstract]. Cardiovasc. Res., 22:589.
- Johnson, A.E., (1979), Force-interval relationship of cardiac muscle. In: Berne M. (ed) Handbook of physiology, sect 2: The cardiovascular system, vol 1, chapter 13. Am Physiol Soc, Bethesda, MA.
- Kentish, J.C., H.E.D.J. ter Keurs, L. Ricciardi, J.J.J. Bucx, and M.I.M Noble, (1986), Comparison between the sarcomere length-force relations of intact and skinned trabeculae from rat right ventricle: influence of calcium concentrations on these relations. Circ. Res., 58:755-768.
- Lakatta, E. G. (1986), length modulation of muscle performance: frank-starling law of the heart. In: H.A. Fozzard et al. (eds) The Heart and Cardiovascular System, pp. 819-841. Raven Press.
- Lakatta, E.G. (1987), Starling's law of the heart is explained by an intimate interaction of muscle length and myofilament calcium activation. J. Am. Coll. Cardiol., 10:1157-1164.
- Lakatta, E.G., and H.A. Spurgeon (1980), Force staircase in mammalian cardiac muscle: modulation by muscle length. J. Physiol., 299:337-352.
- Lakatta, E.G., and D.L. Lappe (1981), Diastolic scattered light fluctuations, resting force and twitch force in mammalian cardiac muscle. J. Physiol., 315:369-394.
- Liu, B., U. Ravens, X-L Wang, and E. Wetter (1988), Studies on isolated myocytes [abstract]. Cardiovasc. Res., 22:590.
- McComb, T.A. (1990), An examination of the force-interval relationship of the chronic diabetic papillary muscle. Independent study, University of Windsor.
- Morad, M., and Y. Goldman (1973) Excitation-contraction coupling in heart muscle: membrane control of development of tension. Prog. Biophys. Molec. Biol., 27:257-313.
- Orchard, C.H., and E.G. Lakatta (1985), Intracellular calcium transients and developed tension and in rat heart muscle: a mechanism for the negative interval-stretch relationship. J. Gen. Physiol., 86:637-651.

- Phillips, P.J., J.K. Gwathmey, M.D. Feldman, F.J. Schoen, W.Grossman and J.P. Morgan (1990), Post-extrasystolic potentiation and the force-frequency relationship: differential augmentation of myocardial contractility in working myocardium from patients with end-stage heart failure. J. Mol. Cell. Cardiol., 22:99-110.
- Pierce, G.N., T.G. Maddaford, E.A. Kroger and E.J. Cragoe (1990), Protection by benzamil against dysfunction and damage in rat myocardium after calcium depletion and repletion. Am. J. Physiol., 258:H17-H23.
- Pogessi, C., R. Bottinelli, M. Vitale, and S. Testa (1984), Postextrasystolic potentiation in isolated rat myocardium: dependence on resting muscle length. Pflugers Arch., 402:321-324.
- Pogessi, C., M. Everts, B. Polla, F. Tanzi, and C. Reggiani (1987), Influence of thyroid state on mechanical restitution of rat myocardium. Circ. Res., 60:142-151.
- Pogessi, C., C. Reggiani, L. Ricciardi, and R. Minelli (1982), Factors modulating the sensitivity of the relaxation to the loading conditions in rat cardiac muscle. Pflugers Arch., 394:338-346.
- Pollack, G.H., and L.L. Huntsman (1974) Sarcomere length-active force relations in living mammalian cardiac muscle. Am. J. Physiol., 227(2):383-389.
- Ragnarsdottir K., B. Wohlfart, and M. Johannson (1982), Mechanical restitution of the rat papillary muscle. Acta Physiol. Scand., 115:183-191.
- Reugg, J.C. (1986), Calcium in Muscle Activation, Springer-Verlag, New York.
- Ridgway, E.B., and A.M. Gordon (1975), Muscle activation: effect of small length changes on calcium release in single fibres. Science, 189:881-883.
- Schouten, V.J.A. (1985), Excitation-contraction coupling in heart muscle, PhD thesis, University of Leiden.
- Schouten, V.J.A., J.K. van Deen, P. de Tombe, and A.A. Verveen (1987), Force-interval relationship in the heart muscle of mammals: a calcium compartment model. Biophys. J., 51:13-26.
- Seed, W.A., and J.M. Walker (1988), Relation between beat interval and force of the heartbeat and its clinical implications. Cardiovasc. Res., 22:303-314.
- Shattock, M.J., and D.M. Bers (1989), Rat vs. Rabbit

ventricle: Ca flux and intracellular Na assessed by ion-selective microelectrodes. Am. J. Physiol., 256:C813-C822.

Siegl, P.K.S., E.J. Cragoe, M.J. Trumble and G.J. Kaczorowski (1984), Inhibition of Na⁺/Ca⁺⁺ exchange in membrane vesicle and papillary muscle preparations from guinea pig heart by analogs of amiloride. Proc. Natl. Acad. Sci., 81:3238-3242.

Sonn, J.K., and C.O. Lee (1988), Na⁺-Ca⁺⁺ exchange in regulation of contractility in canine purkinje fibres. Am. J. Physiol., 255:C278-C290.

Stefanon, I., D.V. Vassallo, and J.G. Mill (1990), Left ventricular length dependent activation in the isovolumetric rat heart. Cardiovascular Res. 24:254-256.

Sutko, J.L., D.M. Bers, and J.P. Reeves (1986), Postrest inotropy in rabbit ventricle: Na⁺-Ca⁺⁺ exchange determines sarcoplasmic reticulum Ca⁺⁺ content. Am. J. Physiol., 250:H654-H661.

Taylor, P.B., R.K. Helbing, S. Rourke, and D. Churchill (1989), Effect of catecholamine-induced cardiac hypertrophy on the force-interval relationship. Can. J. Physiol. Pharmacol., 67:40-46.

ter Keurs, H.E.D.J., W.H. Rijnsburger and R. van Heuningen (1980), Restoring forces and relaxation of rat cardiac muscle. Eur. Heart J., 1:67-80.

ter Keurs, H.E.D.J., W.H. Rijnsburger, R. van Heuningen, and M.J. Nagelsmit, (1980b), Tension development and sarcomere length in rat cardiac trabeculae: evidence of length-dependent activation. Circ. Res., 46:703-714.

ter Keurs, H.E.D.J., V.J.A. Schouten, J.J. Buck, B.M. Mulder, and P.P. de Tombe (1987), Excitation-contraction coupling in myocardium: implications of calcium release and Na⁺ - Ca⁺⁺ exchange. Can. J. Physiol. Pharmacol., 65:619-626.

Tortora, G.J., and R.L. Evans (1986), Principles of Human Physiology, second edition, Harper and Row Publishers, New York.

Wier, W., and Yue, D.T. (1986), Intracellular calcium transients underlying the short term force-interval relationship in ferret ventricular myocardium. J. Physiol., 376:507-530.

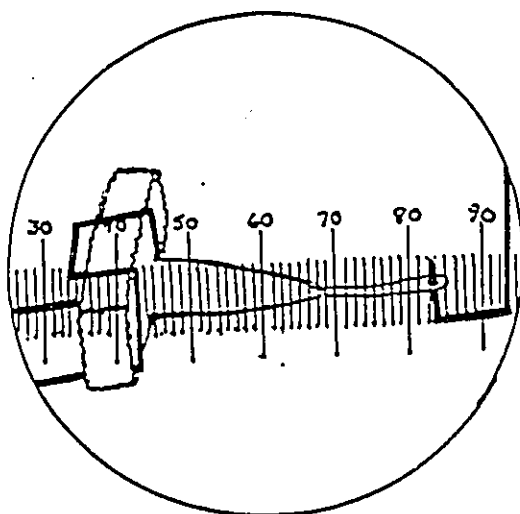
Wohlfart, B., A.F. Grimm, and K.A.P. Edman (1977),

Relationship between sarcomere length and active force in rabbit papillary muscle. Acta Physiol. Scand., 101:155-164.

Yue, D.T. (1987), Intracellular $[Ca^{++}]$ related to rate of force development in twitch contraction of heart. Am. J. Physiol., 252:H760-H770.

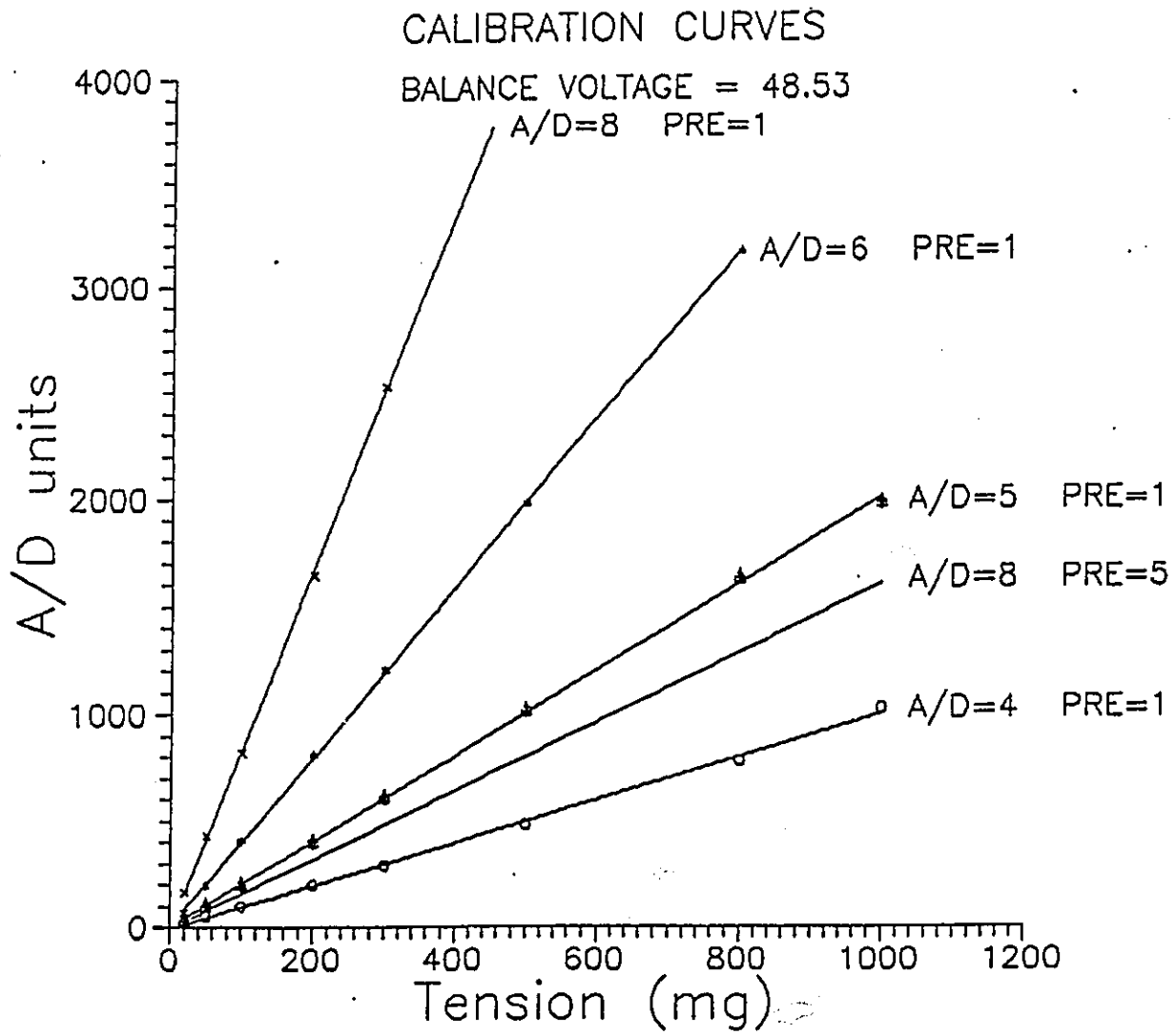
APPENDIX A

Eyepiece reticle scale used in the determination
of muscle lengths



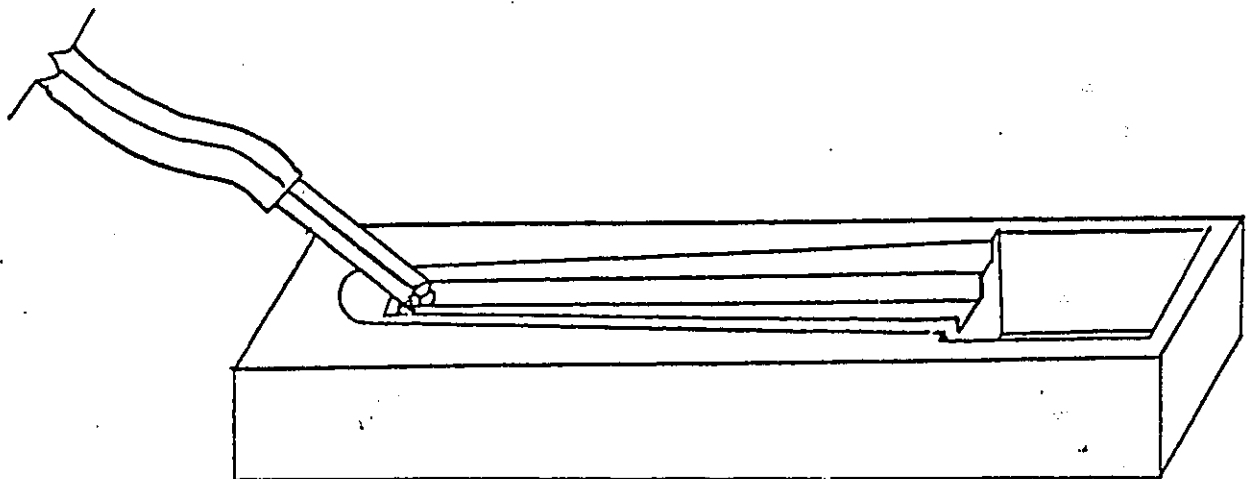
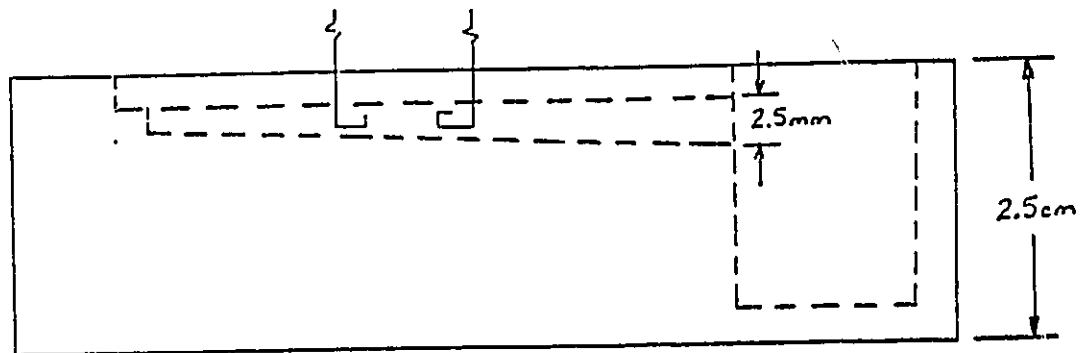
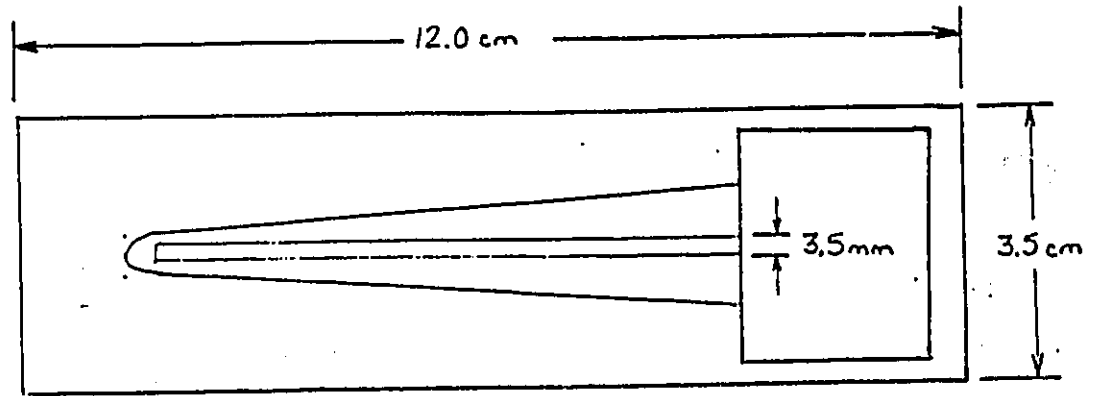
APPENDIX B

Calibration curves generated for force measurements
using the Grass FT03 force transducer



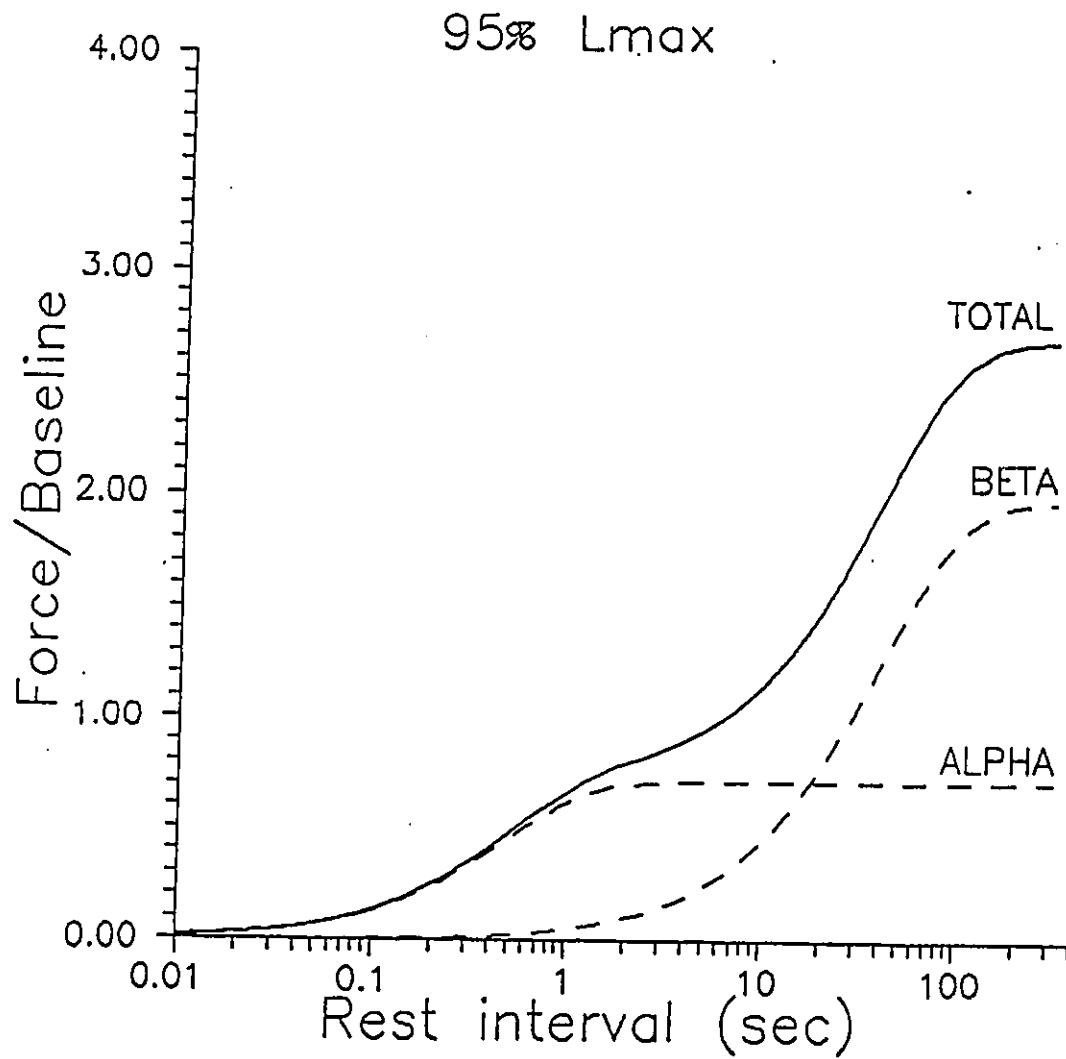
APPENDIX C

Specifications for muscle bath developed for the
quick-exchange buffer experiments



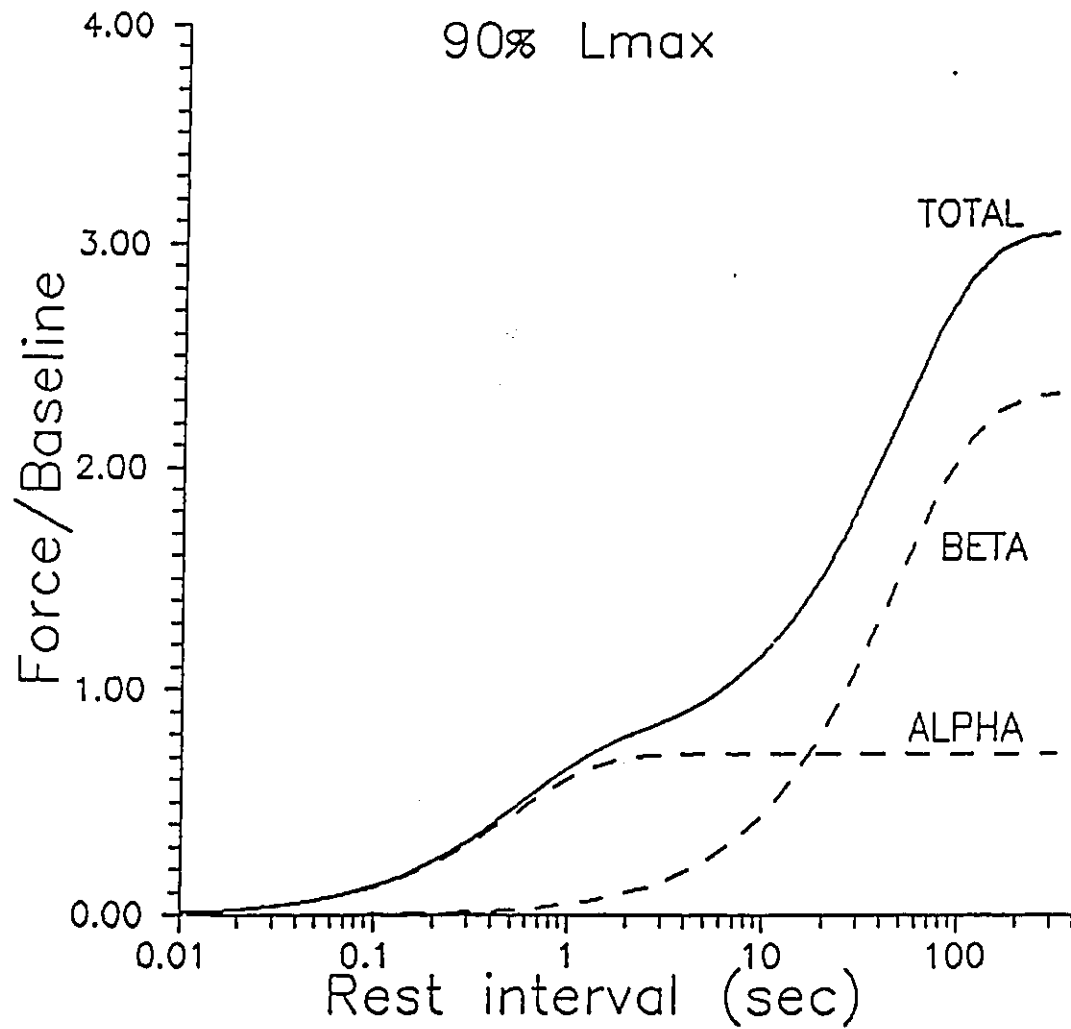
APPENDIX D

Fitted force-interval data at 95% Lmax with mathematically isolated alpha and beta processes



APPENDIX E

Fitted force-interval data at 90% Lmax with mathematically isolated alpha and beta processes



APPENDIX F

Raw force-interval data in right ventricular
papillary muscle of the rat

100% Lmax

Rest time (secs)	Force/baseline values				
	Experiment				
	A	B	C	D	E
0.40	0.7103	0.7806	0.6870	0.6372	0.6921
0.54	0.6968	0.6834	0.6158	0.6001	0.6563
0.73	0.6884	0.6800	0.6274	0.6094	0.6620
0.99	0.7858	0.7143	0.6471	0.6419	0.7167
1.34	0.8542	0.7713	0.7005	0.6983	0.7742
1.81	0.8894	0.8247	0.7609	0.7619	0.8275
2.44	0.9259	0.8729	0.8355	0.8410	0.8923
3.36	0.9596	0.9519	0.9089	0.9053	0.9306
4.46	0.9902	0.9926	0.9618	0.9811	0.9814
6.02	1.0219	1.0172	1.0336	1.0233	1.0000
8.13	1.0519	1.0514	1.0751	1.1047	1.0678
10.47	1.1112	1.0831	1.1400	1.2058	1.1326
14.81	1.1428	1.1359	1.2177	1.3144	1.2019
20.00	1.1936	1.2129	1.2928	1.4499	1.2438
27.00	1.2360	1.2695	1.4208	1.5993	1.3183
36.45	1.2516	1.3084	1.5749	1.7801	1.4189
49.21	1.3302	1.3742	1.7265	1.9284	1.5360
66.44	1.3855	1.4112	1.8610	2.0439	1.6340
89.70	1.4402	1.6293	2.0210	2.0960	1.7431
121.00	1.4872	1.8547	2.1516	2.1411	1.8518
130.00	1.4767	2.0390	2.2230	2.0843	1.9756
135.00	1.4876	2.1260	2.2170	2.0910	2.0343
150.00	1.5099	2.0490	2.1844	2.1182	2.0699
163.00	1.5000	2.0244	2.2921	2.2847	2.1404

APPENDIX G

Raw force-interval data in right ventricular
papillary muscle of the rat

95% Lmax

Rest time (secs)	Force/baseline values				
	Experiment				
	A	B	C	D	E
0.40	0.5260	0.5000	0.5590	0.5342	0.5263
0.54	0.5660	0.5301	0.5862	0.5993	0.5718
0.73	0.5815	0.5769	0.6096	0.6510	0.5779
0.99	0.6502	0.6297	0.6440	0.6844	0.5892
1.34	0.6793	0.7045	0.6900	0.7267	0.6533
1.81	0.7462	0.7677	0.7548	0.8305	0.7208
2.44	0.7877	0.8516	0.8159	0.8550	0.8065
3.36	0.8899	0.8955	0.8873	0.9426	0.8744
4.46	0.9360	0.9676	0.9606	0.9307	0.9602
6.02	1.0056	1.0303	1.0351	1.0076	1.0412
8.13	1.0522	1.1358	1.1181	1.0461	1.0889
10.47	1.1486	1.2324	1.1910	1.0995	1.2122
14.81	1.2048	1.2859	1.3185	1.2015	1.2624
20.00	1.3626	1.4352	1.4546	1.3440	1.3746
27.00	1.5684	1.5602	1.6598	1.5480	1.5000
36.45	1.8069	1.6500	1.8830	1.7766	1.6917
49.21	2.0634	1.7672	2.1526	2.0240	1.8737
66.44	2.4515	1.7967	2.4521	2.3238	2.0193
89.70	2.7535	1.8384	2.7182	2.4549	2.1788
121.00	2.9148	1.8434	3.0018	2.4930	2.3184
130.00	3.0113	1.9425	3.0311	2.6208	2.2835
135.00	2.9966	1.9676	3.0650	2.5812	2.2414
150.00	3.0827	2.2820	3.1667	2.7167	2.1578
163.00	2.9482	2.2160	3.2070	2.5732	2.1329

APPENDIX H

Raw force-interval data in right ventricular
papillary muscle of the rat

90% Lmax

Rest time (secs)	Force/baseline values				
	Experiment				
	A	B	C	D	E
0.40	0.4211	0.5550	0.5230	0.5455	0.5911
0.54	0.4453	0.5812	0.5350	0.5841	0.5968
0.73	0.4966	0.5658	0.5094	0.6215	0.6263
0.99	0.5501	0.6397	0.5508	0.6432	0.6600
1.34	0.6448	0.6932	0.6110	0.6854	0.7009
1.81	0.7298	0.7276	0.6489	0.7845	0.7470
2.44	0.7941	0.8140	0.7329	0.8463	0.8015
3.36	0.8827	0.9137	0.8115	0.8854	0.8839
4.46	0.9679	0.9582	0.9468	0.8688	0.9638
6.02	1.0697	0.9966	1.0089	0.9679	1.0340
8.13	1.1760	1.0369	1.0808	1.0350	1.1034
10.47	1.2989	1.1969	1.1866	1.1389	1.2004
14.81	1.5108	1.3120	1.2073	1.2359	1.3224
20.00	1.7075	1.3964	1.4072	1.4000	1.4600
27.00	1.9789	1.7165	1.4946	1.6302	1.6905
36.45	2.1770	2.0944	1.8353	1.7449	1.9259
49.21	2.3546	2.2799	1.9877	2.0812	2.3192
66.44	2.5067	2.6099	2.3346	2.2022	2.5039
89.70	2.5054	2.9768	2.5865	2.4650	2.9529
121.00	2.5023	3.0446	2.7726	2.4200	3.3544
130.00	2.4121	3.1385	2.7075	2.4052	3.4209
135.00	2.3475	3.3550	2.7551	2.5620	3.5663
150.00	2.3622	3.3462	2.6984	2.7236	3.6526
163.00	2.3027	3.4180	2.9379	2.6550	3.5888

APPENDIX I

Raw data for twitch characteristics in right ventricular
papillary muscle of the rat

100% Lmax

Parameter	A	B	C	D	E
S+ (u/msec)	5.7227	3.4302	3.1737	3.2378	6.5007
S+ (u/msec)	2.7005	2.1799	1.9235	2.2333	3.9324
T0-T2 (msec)	175.0	181.5	180.0	206.7	191.7
T0-T1 (msec)	55.53	49.20	46.62	50.75	63.72
T1-T2 (msec)	119.5	132.3	133.4	155.9	128.0
T3-T2 (msec)	98.75	102.36	114.78	153.65	111.56
T3-T4 (msec)	310.7	263.4	255.7	192.3	271.5
T4-T2 (msec)	409.40	365.40	370.49	345.91	383.08
C.S.A (mm ²)	0.3087	0.1715	0.2058	0.2058	0.2352
Force (mN/mm ²)	42.53	23.95	19.20	48.31	71.62

APPENDIX J

Raw data for twitch characteristics in right ventricular
papillary muscle of the rat

95% Lmax

Parameter	A	B	C	D	E
S+ (u/msec)	3.3709	1.3303	1.9714	1.1760	5.2778
S- (u/msec)	1.9931	1.1296	1.3542	0.9911	3.6593
T0-T2 (msec)	142.7	107.8	154.8	131.2	152.0
T0-T1 (msec)	56.09	54.25	66.16	58.56	55.67
T1-T2 (msec)	86.6	53.5	88.7	72.6	96.3
T3-T2 (msec)	83.42	49.21	87.00	67.83	85.65
T3-T4 (msec)	180.3	105.8	179.1	41.5	198.7
T4-T2 (msec)	263.73	154.97	266.14	209.35	284.32
C.S.A (mm ²)	0.3087	0.1715	0.2058	0.2058	0.2352
Force (mN/mm ²)	9.06	4.53	8.47	4.66	21.54

APPENDIX K

Raw data for twitch characteristics in right ventricular
papillary muscle of the rat

90% Lmax

Parameter	A	B	C	D	E
S+ (u/msec)	2.3389	0.6568	0.9482	0.7076	2.6669
S+ (u/msec)	1.5252	0.6443	0.7387	0.6417	1.9606
T0-T2 (msec)	127.5	107.9	151.9	126.8	112.0
T0-T1 (msec)	58.31	56.87	78.97	60.88	54.67
T1-T2 (msec)	69.2	51.0	73.0	65.9	87.1
T3-T2 (msec)	73.37	45.57	64.71	60.00	54.25
T3-T4 (msec)	134.2	91.2	159.2	117.1	122.5
T4-T2 (msec)	207.55	137.29	223.94	177.06	176.71
C.S.A (mm ²)	0.3087	0.1715	0.2058	0.2058	0.2352
Force (mN/mm ²)	5.49	2.43	4.17	2.65	7.12

APPENDIX L

Raw data for potentiation decay in right ventricular papillary muscle of the rat

100% Lmax

Beat #	Force/baseline values			
	A	B	C	D
1	2.1516	1.8518	1.4872	1.8256
2	1.7102	1.4974	1.3821	1.4267
3	1.4020	1.2623	1.2724	1.1605
4	1.2073	1.1053	1.1891	0.9919
5	1.0698	1.0140	1.1250	
6	0.9817	0.9614	1.0826	
7			1.0558	

95% Lmax

Beat #	Force/baseline values			
	A	B	C	D
1	2.7726	2.4184	2.5023	3.0446
2	1.8082	1.6361	2.0345	2.0633
3	1.3904	1.1922	1.6822	1.5073
4	1.1504	1.0596	1.4474	1.2337
5	1.0170	1.0034	1.2938	1.0731
6	0.9452	0.8503	1.1787	1.0203
7	0.9156	0.8742	1.1338	0.9568

90% Lmax

Beat #	Force/baseline values			
	A	B	C	D
1	2.3178	2.4930	1.8434	2.9148
2	1.7479	1.7210	1.6409	1.8584
3	1.4522	1.3238	1.4342	1.3794
4	1.2623	1.1371	1.2787	1.1112
5	1.1266	1.0112	1.1681	1.0000
6	1.0621	0.9308	1.0856	0.9818
7	1.0239	0.9224	1.0386	0.8938

APPENDIX M

Values chosen for Eureka fitting procedure

$$f(t) = F_{\text{end}} * (1 - M * \exp(-at) - (1 - m) * \exp(-bt))$$

$$A1 = Z * M$$

$$A2 = Z * (1 - M)$$

100% Lmax

A = 1.9995842
B = 0.0195498
M = 0.4834525
Z = 2.0409753

negative differences = 5
maximum error = 0.186684
last error = 1.92

95% Lmax

A = 2.0000020
B = 0.0249649
M = 0.2654680
Z = 2.6801754

negative differences = 10
maximum error = 0.130155
last error = 1.35

90% Lmax

A = 1.9055734
B = 0.0213008
M = 0.2348897
Z = 3.0309166

negative differences = 12
maximum error = 0.115059
last error = 0.76

APPENDIX N

Raw data for buffer exchange experiments in right ventricular papillary muscle of the rat

rest duration = 121.0seconds

Test potentiation 1mM Ca⁺⁺

	Force/baseline values				
	Experiment				
	A	B	C	D	E
100% Lmax	1.564	1.655	1.869	1.666	1.829
90% Lmax	3.354	2.420	2.773	2.502	3.045

Test potentiation 0.5mM Ca⁺⁺

	Force/baseline values					
	Experiment					
	A	B	C	D	E	F
100% Lmax	2.726	2.286	3.549	3.256	2.612	4.865
90% Lmax	4.567	4.426	4.133	5.338		

Swap: 0.5mM Ca⁺⁺ -> 2.5mM Ca⁺⁺

	Force/baseline values			
	Experiment			
	A	B	C	D
100% Lmax	7.986	6.411	4.627	12.744
90% Lmax	10.371	11.552	10.076	22.176

APPENDIX O

Raw data for buffer exchange experiments in right
ventricular papillary muscle of the rat

rest duration = 121.0seconds

Test potentiation 1mM Ca⁺⁺

	Force/baseline values				
	Experiment				
	A	B	C	D	E
100% Lmax	1.571	1.634	1.729	1.826	1.764
90% Lmax	3.354	2.420	2.773	2.502	3.045

Test potentiation 0.5mM Ca⁺⁺

	Force/baseline values					
	Experiment					
	A	B	C	D	E	F
100% Lmax	3.317	4.134	2.294	3.865	2.446	
90% Lmax	5.768	3.693	2.983	4.255	3.421	

Swap: 0.5mM Ca⁺⁺ -> low Na⁺ (40% reduction)

	Force/baseline values			
	Experiment			
	A	B	C	D
100% Lmax	4.113	5.212	4.694	2.833
90% Lmax	7.275	5.524	5.961	4.422

APPENDIX P

Analysis of variance with Fisher PLSD post hoc analyses

Force

One Factor ANOVA-Repeated Measures for X₁ ... X₃

Source:	df:	Sum of Squares:	Mean Square:	F-test:	P value:
Between subjects	4	1057.1988	264.2997	.5438	.7077
Within subjects	10	4859.8397	485.984		
treatments	2	3948.003	1974.0015	17.3189	.0012
residual	8	911.8367	113.9796		
Total	14	5917.0384			

Reliability Estimates for- All treatments: -.8388 Single Treatment: -.1793

One Factor ANOVA-Repeated Measures for X₁ ... X₃

Group:	Count:	Mean:	Std. Dev.:	Std. Error:
TS1	5	41.122	20.9716	9.3788
TS2	5	9.652	6.9683	3.1163
TS3	5	4.372	1.9735	.8826

One Factor ANOVA-Repeated Measures for X₁ ... X₃

Comparison:	Mean Diff.:	Fisher PLSD:	Scheffe F-test:	Dunnett t:
TS1 vs. TS2	31.47	15.5725*	10.8612*	4.6607
TS1 vs. TS3	36.75	15.5725*	14.8115*	5.4427
TS2 vs. TS3	5.28	15.5725	.3057	.782

* Significant at 95%

+ dF/dT

One Factor ANOVA-Repeated Measures for X₁ ... X₃

Source:	df:	Sum of Squares:	Mean Square:	F-test:	P value:
Between subjects	4	26557.1131	6639.2783	1.4128	.2987
Within subjects	10	46993.6651	4699.3665		
treatments	2	43365.775	21682.8875	47.8138	.0001
residual	8	3627.8901	453.4863		
Total	14	73550.7782			

Reliability Estimates for- All treatments: .2922 Single Treatment: .121

One Factor ANOVA-Repeated Measures for X₁ ... X₃

Group:	Count:	Mean:	Std. Dev.:	Std. Error:
TS1	5	191.022	48.7353	21.7951
TS2	5	110.672	64.1329	28.6811
TS3	5	60.472	32.5284	14.5471

One Factor ANOVA-Repeated Measures for X₁ ... X₃

Comparison:	Mean Diff.:	Fisher PLSD:	Scheffe F-test:	Dunnnett t:
TS1 vs. TS2	80.35	31.0618*	17.7958*	5.9659
TS1 vs. TS3	130.55	31.0618*	46.9786*	9.6931
TS2 vs. TS3	50.2	31.0618*	6.9463*	3.7273

* Significant at 95%

- dF/dT

One Factor ANOVA-Repeated Measures for X₁ ... X₃

Source:	df:	Sum of Squares:	Mean Square:	F-test:	P value:
Between subjects	4	10847.2363	2711.8091	2.0111	.1688
Within subjects	10	13484.2368	1348.4237		
treatments	2	11558.1767	5779.0884	24.0038	.0004
residual	8	1926.06	240.7575		
Total	14	24331.4731			

Reliability Estimates for- All treatments: .5028 Single Treatment: .2521

One Factor ANOVA-Repeated Measures for X₁ ... X₃

Group:	Count:	Mean:	Std. Dev.:	Std. Error:
TS1	5	114.5358	31.4785	14.0776
TS2	5	78.47	42.0969	18.8263
TS3	5	46.584	20.7432	9.2766

One Factor ANOVA-Repeated Measures for X₁ ... X₃

Comparison:	Mean Diff.:	Fisher PLSD:	Scheffe F-test:	Dunnett t:
TS1 vs. TS2	36.0658	22.6326*	6.7534*	3.6752
TS1 vs. TS3	67.9518	22.6326*	23.9735*	6.9244
TS2 vs. TS3	31.886	22.6326*	5.2787*	3.2492

* Significant at 95%

S+/S- ratio

One Factor ANOVA-Repeated Measures for X₁ ... X₃

Source:	df:	Sum of Squares:	Mean Square:	F-test:	P value:
Between subjects	4	.5723	.1431	2.7276	.0903
Within subjects	10	.5246	.0525		
treatments	2	.483	.2415	46.4549	.0001
residual	8	.0416	.0052		
Total	14	1.0969			

Reliability Estimates for- All treatments: .6334 Single Treatment: .3654

One Factor ANOVA-Repeated Measures for X₁ ... X₃

Group:	Count:	Mean:	Std. Dev.:	Std. Error:
TS1	5	1.6858	.2569	.1149
TS2	5	1.3902	.2136	.0955
TS3	5	1.2563	.2046	.0915

One Factor ANOVA-Repeated Measures for X₁ ... X₃

Comparison:	Mean Diff.:	Fisher PLSD:	Scheffe F-test:	Dunnett t:
TS1 vs. TS2	.2956	.1052*	21.0119*	6.4826
TS1 vs. TS3	.4295	.1052*	44.3591*	9.419
TS2 vs. TS3	.1339	.1052*	4.3114	2.9365

* Significant at 95%

T0-T1 100 95 90%Lmax

One Factor ANOVA-Repeated Measures for X₁ ... X₃

Source:	df:	Sum of Squares:	Mean Square:	F-test:	P value:
Between subjects	4	176.8257	44.2064	.6587	.6344
Within subjects	10	671.0989	67.1099		
treatments	2	193.7216	96.8608	1.6232	.256
residual	8	477.3774	59.6722		
Total	14	847.9246			

Reliability Estimates for- All treatments: -.5181 Single Treatment: -.1284

One Factor ANOVA-Repeated Measures for X₁ ... X₃

Group:	Count:	Mean:	Std. Dev.:	Std. Error:
TS1	5	53.164	6.7341	3.0116
TS2	5	58.146	4.7416	2.1205
TS3	5	61.94	9.7836	4.3754

One Factor ANOVA-Repeated Measures for X₁ ... X₃

Comparison:	Mean Diff.:	Fisher PLSD:	Scheffe F-test:	Dunnett t:
TS1 vs. TS2	-4.982	11.2676	.5199	1.0197
TS1 vs. TS3	-8.776	11.2676	1.6134	1.7963
TS2 vs. TS3	-3.794	11.2676	.3015	.7766

T0-T2 100-95-90%Lmax

One Factor ANOVA-Repeated Measures for X₁ ... X₃

Source:	df:	Sum of Squares:	Mean Square:	F-test:	P value:
Between subjects	4	1468.7667	367.1917	.2942	.8752
Within subjects	10	12481.3667	1248.1367		
treatments	2	10664.2773	5332.1387	23.4755	.0004
residual	8	1817.0893	227.1362		
Total	14	13950.1333			

Reliability Estimates for- All treatments: -.2399 Single Treatment: -.3076

One Factor ANOVA-Repeated Measures for X₁ ... X₃

Group:	Count:	Mean:	Std. Dev.:	Std. Error:
TS1	5	186.98	12.584	5.6277
TS2	5	137.7	19.0929	8.5386
TS3	5	125.22	17.2791	7.7274

One Factor ANOVA-Repeated Measures for X₁ ... X₃

Comparison:	Mean Diff.:	Fisher PLSD:	Scheffe F-test:	Dunnett t:
TS1 vs. TS2	49.28	21.983*	13.3649*	5.1701
TS1 vs. TS3	61.76	21.983*	20.9912*	6.4794
TS2 vs. TS3	12.48	21.983	.8571	1.3093

* Significant at 95%

T1-T2

One Factor ANOVA-Repeated Measures for X₁ ... X₃

Source:	df:	Sum of Squares:	Mean Square:	F-test:	P value:
Between subjects	4	1091.9533	272.9883	.2023	.9314
Within subjects	10	13493.1667	1349.3167		
treatments	2	12038.308	6019.154	33.0982	.0001
residual	8	1454.8587	181.8573		
Total	14	14585.12			

Reliability Estimates for- All treatments: -.3.943 Single Treatment: -.3622

One Factor ANOVA-Repeated Measures for X₁ ... X₃

Group:	Count:	Mean:	Std. Dev.:	Std. Error:
TS1	5	133.82	13.4995	6.0372
TS2	5	79.54	16.8885	7.5528
TS3	5	69.24	13.0093	5.818

One Factor ANOVA-Repeated Measures for X₁ ... X₃

Comparison:	Mean Diff.:	Fisher PLSD:	Scheffe F-test:	Dunnett t:
TS1 vs. TS2	54.28	19.6702*	20.2516*	6.3642
TS1 vs. TS3	64.58	19.6702*	28.6665*	7.5719
TS2 vs. TS3	10.3	19.6702	.7292	1.2077

* Significant at 95%

T3-T2

One Factor ANOVA-Repeated Measures for X₁ ... X₃

Source:	df:	Sum of Squares:	Mean Square:	F-test:	P value:
Between subjects	4	1363.0076	340.7519	.3199	.8584
Within subjects	10	10652.4791	1065.2479		
treatments	2	8607.9083	4303.9541	16.8405	.0014
residual	8	2044.5709	255.5714		
Total	14	12015.4868			

Reliability Estimates for- All treatments: -.2.126 Single Treatment: -.2932

One Factor ANOVA-Repeated Measures for X₁ ... X₃

Group:	Count:	Mean:	Std. Dev.:	Std. Error:
TS1	5	116.22	21.9208	9.8033
TS2	5	74.622	16.1566	7.2254
TS3	5	59.58	10.5041	4.6976

One Factor ANOVA-Repeated Measures for X₁ ... X₃

Comparison:	Mean Diff.:	Fisher PLSD:	Scheffe F-test:	Dunnett t:
TS1 vs. TS2	41.598	23.3185*	8.4634*	4.1142
TS1 vs. TS3	56.64	23.3185*	15.6908*	5.6019
TS2 vs. TS3	15.042	23.3185	1.1066	1.4877

* Significant at 95%

T2-T4

One Factor ANOVA-Repeated Measures for X₁ ... X₃

Source:	df:	Sum of Squares:	Mean Square:	F-test:	P value:
Between subjects	4	12281.1048	3070.2762	.299	.872
Within subjects	10	102672.3983	10267.2398		
treatments	2	97026.7605	48513.3802	68.7446	.0001
residual	8	5645.6378	705.7047		
Total	14	114953.5031			

Reliability Estimates for- All treatments: -2.344 Single Treatment: -.3049

One Factor ANOVA-Repeated Measures for X₁ ... X₃

Group:	Count:	Mean:	Std. Dev.:	Std. Error:
TS1	5	374.856	23.4908	10.5054
TS2	5	235.702	53.1221	23.7569
TS3	5	184.51	33.2853	14.8856

One Factor ANOVA-Repeated Measures for X₁ ... X₃

Comparison:	Mean Diff.:	Fisher PLSD:	Scheffe F-test:	Dunnett t:
TS1 vs. TS2	139.154	38.7485*	34.2988*	8.2824
TS1 vs. TS3	190.346	38.7485*	64.1763*	11.3293
TS2 vs. TS3	51.192	38.7485*	4.6419*	3.0469

* Significant at 95%

T3-T4

One Factor ANOVA-Repeated Measures for X₁ ... X₃

Source:	df:	Sum of Squares:	Mean Square:	F-test:	P value:
Between subjects	4	17955.884	4488.971	.7164	.5996
Within subjects	10	62659.84	6265.984		
treatments	2	53377.936	26688.968	23.003	.0005
residual	8	9281.904	1160.238		
Total	14	80615.724			

Reliability Estimates for- All treatments: -.3959 Single Treatment: -.1044

One Factor ANOVA-Repeated Measures for X₁ ... X₃

Group:	Count:	Mean:	Std. Dev.:	Std. Error:
TS1	5	258.72	42.7431	19.1153
TS2	5	141.08	66.0769	29.5505
TS3	5	124.84	24.8257	11.1024

One Factor ANOVA-Repeated Measures for X₁ ... X₃

Comparison:	Mean Diff.:	Fisher PLSD:	Scheffe F-test:	Dunnett t:
TS1 vs. TS2	117.64	49.6841 *	14.9098*	5.4607
TS1 vs. TS3	133.88	49.6841 *	19.3105*	6.2146
TS2 vs. TS3	16.24	49.6841	.2841	.7538

* Significant at 95%

VITA AUCTORIS

NAME: James Gamble

PLACE OF BIRTH: Toronto, Ontario

YEAR OF BIRTH: 1965

EDUCATION: North Albion Collegiate Institute,
Toronto, Ontario
1980-1984 SSHGD

York University, North York, Ontario
1984-1988 Hons. B.Sc.

University of Windsor, Windsor, Ontario
1988-1990 M.H.K.